

UNIVERSIDADE DE LISBOA
FACULDADE DE CIÊNCIAS
DEPARTAMENTO DE BIOLOGIA ANIMAL



Immunogenicity and tumour microenvironment in the zebrafish xenograft model

Mariana Maia Gil

Mestrado em Biologia Evolutiva e do Desenvolvimento

Dissertação orientada por:
Rita Fior, PhD
Gabriela Rodrigues, PhD

2017

Acknowledgements

Imensogeticity and thesis amazingenvironment in the Fiofish xenograft lab

Gostaria de deixar um sincero obrigado a todos aqueles que, de algum modo, me acompanharam durante este percurso:

Sem mais, queria agradecer a todos os elementos do mestrado de Biologia Evolutiva e do Desenvolvimento da Faculdade de Ciências da Universidade de Lisboa pelo excelente ambiente e por todas as oportunidades de aprendizagem - o sucesso deste mestrado parte da dedicação e excelência dos seus professores.

Gostaria de agradecer à minha orientadora Rita Fio pelo sistemático, académico e pessoal, apoio e, principalmente, por me ter dado as ferramentas e a liberdade necessárias à minha aprendizagem de como pensar e fazer Ciência. Foi um privilégio ter o teu exemplo durante este percurso. Obrigada!

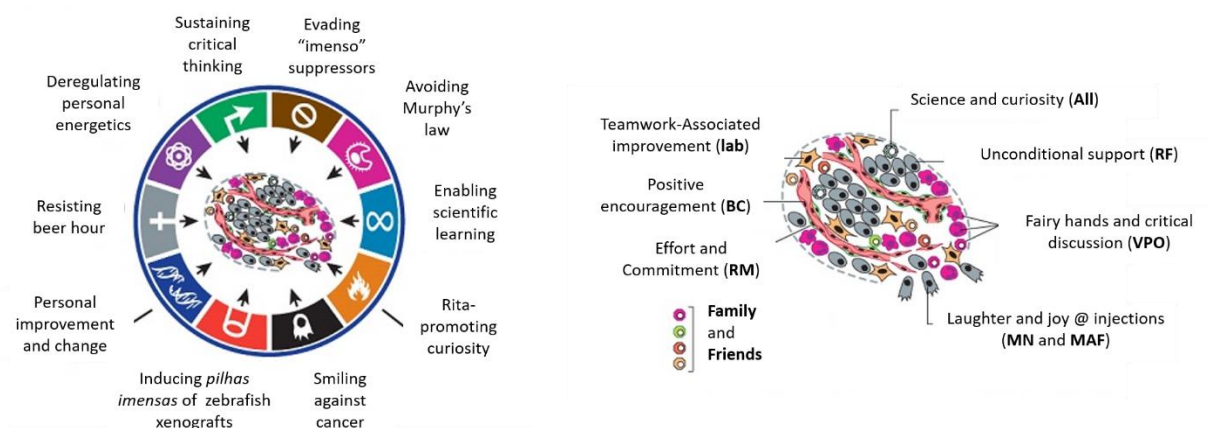
Gostaria de agradecer à minha orientadora Gabriela Rodrigues pela sua disponibilidade e apoio durante este ano e todos os anos em que tive a alegria de ser sua aluna.

Um obrigada muito especial à Vanda Póvoa por me ter ensinado tudo o que lhe foi possível e pela sua incessante ajuda. O teu folêgo e entusiasmo vão, sem dúvida, proporcionar fantásticos caminhos a este projecto.

Obrigada a todo o laboratório do IGC e, em especial, ao Miguel Godinho Ferreira pela produtiva discussão científica. Muito obrigada Raquel, por toda a tua paciência e disponibilidade para as minhas, nem sempre simples, constantes perguntas. Obrigada Bruna pelo teu apoio nesta recta final – transmites confiança mostrando que sabes o que fazes e, sobretudo, porque o fazes. Um obrigada à princesa Magda por este grande caminho. Um brinde à Mafalda, por toda a amizade. Obrigada também a todos aqueles com quem tive o privilégio de “partilhar ciência” durante este ano: Miguel Fuzeta, Ana Logrado, Inês Tenente e Mariana Oliveira. Susana, Cátia e Mariana: aproveitem! Obrigada também ao staff da fish facility da CCU – Catarina Certal, Sandra Martins, Joana Monteiro e Telma Costa – e da flow cytometry – Ana Vieira – pela disponibilidade, ajuda e boa disposição.

Um abraço apertado a toda a minha família e aos meus amigos. E um especial beijinho ao grande Tio Tonecas, Becherovska!

“Querida mãe, querido pai, então que tal?”



Hallmarks of my master thesis – acquired capabilities and their facilitators (left) & major parameters of this thesis amazing-environment (right) – which make me very grateful to the Fio lab.

Resumo

A incidência e a prevalência do cancro têm vindo a aumentar, sendo que, actualmente, o cancro representa uma das maiores causas de morte a nível mundial. As terapêuticas para esta doença focam-se nos diferentes “*hallmarks of cancer*”, isto é, actuam sobre características biológicas particulares às células tumorais. Dentro destas, o microambiente tumoral tem ganho relevo, com um foco maior nas células do sistema imunitário que o compõem. Embora as células imunitárias sejam um dos principais constituintes dos TME, a resposta imunitária anti-cancro encontra-se muitas vezes suprimida. Deste modo, as imunoterapias actuam não sobre as células tumorais *per se*, mas visam atenuar a resposta imunitária, para combater o cancro.

As interacções entre as células do sistema imunitário e as células tumorais são dinâmicas e preponderantes à progressão tumoral. O sistema imunitário reconhece e elimina frequentemente células cancerígenas. No entanto, algumas subpopulações tumorais não são reconhecidas/eliminadas pelo sistema imune, permanecendo no tecido. Isto pode levar à formação de tumores pouco imunogénicos, isto é, que não induzem uma resposta imunitária. Advém a ideia de que, resultante da acção do sistema imunitário, os tumores são seleccionados relativamente à sua imunogenicidade. Entre outras, as experiências de Schreiber *et al.* tiveram como objectivo perceber o efeito do sistema imunitário no desenvolvimento e na progressão tumoral. Para tal, carcinogénicos químicos foram injectados em ratos imunocompetentes (WT) e em ratos imunodeficientes (Rag2^{-/-}). Os autores observaram que a taxa de formação de tumores em ratos imunocompetentes foi muito baixa, o que contrastou com uma maior eficiência em ratos imunodeficientes. Estes resultados sugerem que o sistema imune previne a formação de tumores, processo denominado por “*immune surveillance*”. Numa experiência consequente, os tumores que cresceram em ratos WT e em ratos Rag2^{-/-} foram injectados em ratos imunocompetentes (WT). Curiosamente, os poucos tumores provenientes de ratos WT (que já tinham sido seleccionados relativamente à sua imunogenicidade, “editados”) conseguiram implantar com maior eficiência em ratos com o sistema imunitário competente (100% de implantação). No entanto, os tumores provenientes de ratos Rag2^{-/-} (que ainda não foram sujeitos à pressão selectiva do sistema imunitário, “não editados”) não foram tão eficientes a implantar quando sujeitos à acção do sistema imunitário (50% de implantação). Esta experiência sugere que a interacção entre as células do sistema imunitário e as células tumorais é crucial à progressão tumoral num hospedeiro imuno competente. Para além disto, estas experiências sugerem ainda que o estudo da capacidade de implantação de diferentes tumores poderá ajudar a perceber o papel do sistema imunitário na progressão tumoral.

Recentemente o peixe-zebra demonstrou ser um bom modelo para xenotransplantar tumores humanos, mostrando ter resolução suficiente para diferenciar a capacidade de implantação de linhas tumorais derivadas do mesmo paciente. Diversos trabalhos em peixes-zebra têm demonstrado a sua eficiência para estudar a interacção de células tumorais com células do sistema imunitário através de microscopia em tempo real.

Em estudos anteriores do laboratório, duas linhas celulares de cancro colo-rectal provenientes do mesmo paciente foram injectadas em larvas de peixe-zebra. Enquanto as células SW480 (que derivaram do tumor primário) são frequentemente rejeitadas do hospedeiro, as SW620 (que derivaram de uma metástase nos gânglios linfáticos) têm uma grande capacidade de implantação. O MIX (co-injecção de SW480+SW620, num rácio de 1:1) apresenta uma capacidade de implantação intermédia entre as SW480 e as SW620. Observou-se também que, no MIX, a capacidade de proliferação das SW480 aumenta e a apoptose das células SW620 diminui, sugerindo que estas células estabelecem uma interacção de cooperação *in vivo*.

Para além da capacidade de implantação das SW480 aumentar quando estas são co-injectadas com as SW620 (“MIX”), esta também aumenta quando as SW480 são injectadas em larvas de peixes-

zebra nas quais o desenvolvimento do sistema imunitário inato foi comprometido (após injeção de Pu.1 morfolino). Estes resultados sugerem que a linha celular SW620 poderá ter um papel imunossupressor que lhe confere a capacidade de implantação. Consequentemente, o grande objectivo deste trabalho é perceber “Qual é o mecanismo responsável pelo processo de implantação/rejeição?”.

Para estudar a interacção entre as SW480, as SW620 e o peixe-zebra, foi primeiro testado se as interacções de cooperação entre estas células (aumento de proliferação e diminuição de apoptose) são um resultado de propriedades intrínsecas dos tumores (*tumour-autonomous*), ou se dependem do hospedeiro (*non-tumour-autonomous*). Como tal, as células SW480 e SW620 foram mono- e co-cultivadas *in vitro*. Se a cooperação observada fosse resultado de propriedades intrínsecas dos tumores, então o mesmo fenótipo de proliferação e apoptose em co-cultura *in vitro* deveria ser observado. Contudo, não foram observadas diferenças nos comportamentos das células entre mono- e co-cultura, sugerindo que a cooperação observada *in vivo* é dependente do hospedeiro.

Os resultados de cooperação obtidos relativamente à proliferação e à apoptose são referentes a tumores implantados, no final do ensaio. Como a diminuição da implantação tumoral é um processo dinâmico e contínuo, para perceber os mecanismos envolvidos na implantação/rejeição é necessário analisar estas características num *time-point* inicial e ao longo do tempo. No entanto, as diferenças observadas tanto ao nível de proliferação como de apoptose não explicam as diferentes capacidades de implantação/rejeição. O facto da capacidade de implantação das SW480 aumentar na ausência do sistema imunitário inato sugere que a capacidade de implantação/rejeição pode ser mediada por neutrófilos e/ou macrófagos, uma vez que são as células mais abundantes do sistema imunitário neste estadio de desenvolvimento do peixe.

Para caracterizar a interacção entre as linhas celulares SW480 e SW620 com o sistema imunitário inato, estas linhas tumorais foram injectadas em peixes-zebra transgénicos, com os neutrófilos ou os macrófagos a expressar marcadores fluorescentes, permitindo a sua quantificação no microambiente tumoral. Os resultados indicam que o microambiente tumoral das SW620 é composto por uma maior percentagem de macrófagos comparativamente à de neutrófilos. Em contraste, o microambiente tumoral das SW480 apresenta mais neutrófilos do que o das SW620. Curiosamente, o microambiente tumoral do MIX apresenta valores intermédios, sugerindo que as subpopulações tumorais podem ter sinais contrários. Apesar de o número de neutrófilos não parecer estar associado com a rejeição, verificou-se um aumento destas células no microambiente tumoral das SW620 durante o processo de implantação, sugerindo uma possível função pro-tumoral dos neutrófilos em resposta à metástase. Para além disto, enquanto o número de neutrófilos é independente do número total de células SW480, é dependente do número de células SW620, apontando para diferentes comportamentos dos neutrófilos em resposta às duas subpopulações.

Durante o processo de “*tumour immunoediting*” há uma selecção que leva à progressão de tumores pouco imunogénicos. Estes tumores “editados” conseguem escapar ao controlo do sistema imunitário, tendo uma maior capacidade de implantação em hospedeiros imunocompetentes. Considerando esta premissa, os resultados de implantação deste trabalho permitem associar as condições SW480-MIX-SW620 como três estados consecutivos de progressão tumoral, que podem representar uma história de evolução clonal. Durante a progressão tumoral, o tumor primário, SW480, que apresenta uma baixa implantação, poderá ter adquirido uma nova subpopulação, as SW620. A co-existência das duas subpopulações é representada pelo “MIX” que tem uma capacidade de implantação intermédia. A subpopulação SW620 terá posteriormente adquirido a capacidade de metastizar, apresentando a maior capacidade de implantação e, como tal, o maior “fitness”. Esta subpopulação parece ter a capacidade de escapar ao controlo do sistema imunitário.

Este trabalho mostra diferenças quantitativas relativamente à população de neutrófilos no TME, sugerindo que os neutrófilos possam ter funções diferentes. Para além disto, a estratégia utilizada permite inferir mecanismos imunitários associados à progressão tumoral. Deste modo, o sistema

imunitário inato pode ser um novo alvo complementar às actuais imunoterapias focadas apenas no sistema imune adaptativo. Uma vez que a implantação de tumores humanos em peixes-zebra parece ser mediada por neutrófilos e macrófagos, ao modular estas populações no peixe zebra poder-se-á melhorar a eficácia da implantação de xenotrasplantes de tumores humanos neste modelo animal. Como esta técnica visa ser usada para discriminar qual a quimioterapêutica mais eficiente para cada paciente, aumentar as taxas de sucesso desta técnica poderá contribuir para uma melhor eficiência da medicina personalizada.

Palavras-chave

Cancro Colo-rectal; Xenotransplantes; Peixe-zebra; Microambiente tumoral

Abstract

Cancer develops through a dynamic cross-talk between tumour and immune cells. Within an heterogeneous tumour, while the more immunogenic tumour subpopulations may be cleared, the subpopulations less recognised by the immune system or that create an immunosuppressive microenvironment may remain in the host. These subpopulations can evade immunity, leading to the progression of a low immunogenic tumour. Preliminary data from our laboratory showed that two colorectal cancer cell lines derived from the same patient have contrasting capacities to engraft in the zebrafish larvae. The poor engraftment of SW480 (primary-tumour-derived) is enhanced in the presence of SW620 (lymph-node metastasis-derived) which implant efficiently. Interestingly, when co-injected, these tumour subclones establish an *in vivo* cooperative interaction, where SW480 proliferation increases and SW620 apoptosis reduces. The engraftment of SW480 is also increased when the myeloid cellular compartment of the zebrafish larvae is genetically suppressed. These exciting results drive the main question of this thesis “What is the mechanism behind implantation/rejection capacity?” and prompted us to study the interactions between SW480, SW620 and the host innate immunity.

After confirming the previous preliminary data, we asked whether the observed cooperative interaction regarding proliferation and apoptosis was tumour-autonomous or host dependent. To test this SW480 and SW620 were mono or co-cultured *in vitro*. However, the cooperative effect was no longer observed *in vitro*, suggesting that cooperation is host dependent and therefore we focused on studying the *in vivo* interactions. We started by analysing engraftment/rejection along time and observed different dynamics between conditions from the first moments *in vivo*. Thus, to understand the mechanisms behind it, we analysed xenografts at different time-points including tumours that will engraft and that will be host-rejected. Our results suggested that neither proliferation nor apoptosis are able to modulate engraftment and therefore, the next step was to characterise the neutrophil and macrophage populations in the tumour microenvironment (TME). For this, SW480, SW620 and MIX were injected in transgenic zebrafish with these specific myeloid cells fluorescently labelled. We found that the TME of SW480 has a higher percentage of neutrophils when compared to the TME of SW620. At 1day post-injection (dpi), the MIX TME presents an intermediate percentage of neutrophils, suggesting that SW480 and SW620 may generate conflicting signals regarding neutrophil recruitment. Moreover, only regarding SW620, it was observed that the number of neutrophils in the TME increases along time and is dependent on the number of tumour cells. Concluding, these results suggest that, not only SW480 rejection is independent of neutrophil numbers, but also that neutrophils may acquire a different function in response to SW620, with a possible pro-tumoural effect favouring engraftment.

The tumour-immunoediting process drives the progression of a low immunogenic tumour, which parallels Darwinian evolution. These “edited” tumours can evade the immune system, being able to engraft in immunocompetent hosts. Following, tumour engraftment rates may be a surrogate of tumour’s immunogenicity and thus of tumour progression, meaning that engraftment capacity may be a proxy of tumour fitness. Under this hypothesis, our engraftment results suggest that the SW620 subpopulation appeared in the SW480 primary tumour and further derived metastatisation.

Understanding these intricate interactions between tumour subclones and innate immunity may lead to new avenues of anti-cancer therapies targeting the innate immune component, complementing current adaptive immunotherapies. In contrast, if neutrophils and macrophages play a role in implantation success, modulation of these cells may improve implantation rates of zebrafish patient derived xenografts (zPDXs) as a screening platform for precision medicine.

Key-words

Colorectal cancer; Tumour-immunoediting; Zebrafish; Xenotransplants; Tumour microenvironment

Contents

Acknowledgements.....	i
Resumo	iii
Palavras-chave	v
Abstract.....	vi
Key-words.....	vi
Figure index	ix
1. Introduction.....	1
1.1 Cancer	1
1.2 Cancer Heterogeneity and clonal evolution	1
1.3 Tumour microenvironment	1
1.4 From immune surveillance to immune escape.....	3
1.5 Zebrafish as a model to study tumour implantation/rejection.....	3
1.6 Zebrafish immune system	4
1.7 Studying tumour-immune cells interactions using the zebrafish model	5
2. Results.....	7
2.1 SW620 prevents SW480 rejection and both cooperate to increase tumour proliferation and survival.....	7
2.2 SW480 and SW620 cooperative interactions seem to be non-tumour-autonomous	9
2.3 Tumour clearance over time	10
2.4 SW480 and SW620 present different and dynamic behaviours in vivo since the first 24hours .	11
2.5 SW480 recruits higher number of neutrophils than SW620	13
2.6 The number of neutrophils in the TME does not correlate with tumour rejection.....	14
2.7 Two distinct mechanisms of tumour cells-neutrophils interaction	15
2.8 Characterization of macrophage populations in TME	16
2.9 Modulation of zebrafish larvae innate immune system	17
3. Discussion.....	19
3.1 A history of clonal evolution according to immunoediting theory	22
3.2 Future Work	23
1. Test the immunoediting concept in SW480 cells.....	23
2. Myeloid tumour microenvironment characterisation in vivo.....	23
3. Neutrophil and macrophage immunomodulation.....	23
4. Transcriptome analysis	24
4. Materials and Methods.....	25
4.1 Experimental outline.....	25
4.2 Cell Culture	25

4.2.1 Thawing and expansion of cells.....	25
4.2.2 Labelling of cell lines.....	26
4.3 Zebrafish care and handling.....	26
4.3.1 Crossing and housing of adult zebrafish and embryo harvesting.....	26
4.4 Experiments - in vitro assay.....	26
4.4.1 Seeding.....	26
4.4.2 Immuno fluorescence technique	26
4.5 Experiments - Injections of tumour cells in zebrafish larvae.....	27
4.5.1 Zebrafish Xenografts.....	27
4.5.2 Whole-mount immunofluorescence	27
4.6 Confocal Microscopy.....	27
4.7 Statistical analysis.....	28
4.8 Experiments - Immune suppressor screen	28
4.8.1 Zebrafish larvae drug administration	28
4.8.2 Flow cytometry analysis	28
5. References.....	29

Figure index

Figure 1.1 Zebrafish haematopoiesis has two haematopoietic waves.	4
Figure 1.2 Zebrafish haematopoiesis during larvae development is regulated by different transcriptional genes	5
Figure 1.3 Unravelling the mechanism behind engraftment efficiency	6
Figure 2.1.1 Engraftment analysis of a pair of human CRC cell lines zebrafish-xenografts	7
Figure 2.1.2 SW480 proliferation increases in the presence of SW620 and SW620 apoptosis decreases in the presence of SW480 at 4dpi.	8
Figure 2.2 SW480 and SW620 do not seem to interact in vitro	9
Figure 2.3 Tumour clearance is a continuous process and differs between tumour cell lines derived from the same patient.	10
Figure 2.4.1 SW480 and SW620 present different behaviours after 24hours in vivo	11
Figure 2.4.2 The in vivo SW480 and SW620 behaviour along time is a dynamic process	13
Figure 2.5 Neutrophil populations is higher at SW480 TME	14
Figure 2.6 SW620 TME neutrophil populations raise during tumour selection but it is always lower than SW480 TME neutrophil populations	15
Figure 2.7 Correlative analysis of neutrophils vs total tumour cells	15
Figure 2.8 SW620 TME macrophage populations along time	16
Figure 2.9 Quantification of zebrafish innate immune populations by flow cytometry	17
Figure 3.1 Working hypothesis to unravel the mechanism behind engraftment	21
Figure 3.2 SW480, SW620 and MIX may represent a story of clonal evolution	22
Figure 4.1 Experimental outline	25

Abbreviations

AGM	Aorta-gonad-mesonephros
ATCC	American Type Culture Collection
CAFs	Cancer-Associated Fibroblasts
CHT	Caudal Hematopoietic Tissue
CLP	Common lymphoid progenitor
CMP	Common myeloid progenitor
CRC	Colorectal Cancer
DAPI	4',6-diamidino-2-phenylindole
DAMPs	Damage-associated molecular pattern
DMEM	Dulbecco's Modified Eagle Medium
DMSO	Dimethyl sulfoxide
DPBS	Dulbecco's Phosphate-Buffered Saline
dpf	Days post fertilization
dpi	Days post injection
dps	Days post seeding
ECM	Extracellular Matrix
EMT	Epithelial-mesenchymal transition
FBS	Fetal Bovine Serum
GFP	Green Fluorescent Protein
hpf	Hours post fertilisation
hpi	Hours post injection
HSC	Haematopoietic stem cell
ICM	Intermediate cell mass
irf8	Interferon regulatory factor 8
MHC	Major Histocompatibility Complex
MO	Morpholino
mpeg	Macrophage-expressed gene
mpx	Myeloid-specific peroxidase
n	Number of samples
ns	Not significant (statistically)

P	P-value
PBI	Posterior blood island
PBS	Phosphate-Buffered Saline
PFA	Paraformaldehyde
PVS	Periviteline Space
RBI	Rostral blood island
ROS	Reactive oxygen species
Runx1	Runt-related transcription factor 1
SEM	Standard Error of the Mean
TAMs	Tumour-Associated Macrophages
TANs	Tumour-Associated Neutrophils
TGF- β	Transforming Growth Factor Beta
TME	Tumour Microenvironment
VEGF	Vascular Endothelial Growth Factor
zPDX	Zebrafish Patient-Derived Xenografts

1. Introduction

1.1 Cancer

Healthy multicellular organisms are highly organised systems under precise rules to guarantee their correct development. As a consequence of both external agents and/or inherited genetic factors, cancer cells can break those rules and go through uncontrolled growth, often invading surrounding tissues and metastasising to distant sites. During this process, tumour cells acquire distinct and complementary capabilities that enable tumour growth and metastatic dissemination – known as “hallmarks of cancer”¹. Among those capacities, cancer cells can:

- sustain chronic proliferation and evade growth suppressors, becoming masters of their own destiny;
- activate mechanisms of invasion and metastasis, that are broadly regulated by epithelial-mesenchymal transition (EMT) program;
- develop a variety of strategies to limit or circumvent apoptosis, resisting cell death;
- induce angiogenesis to guarantee their viability;
- maintain telomeric DNA at lengths sufficient to avoid senescence or apoptosis, enabling replicative immortality;
- deregulate cellular energies and
- avoid immune destruction¹.

1.2 Cancer Heterogeneity and clonal evolution

Cancer hallmarks vary from cancer to cancer (inter-tumour heterogeneity). Most tumours are a heterogeneous mass of cells, composed by distinct subpopulations, which can express distinct biological traits (intra-tumour heterogeneity)². These tumour subpopulations appear during cancer development, having evolved by clonal evolution – ie tumours may have originated from a single cell that, due to different factors, acquired some advantage, leading to uncontrolled proliferation³. This proliferative environment prompts cells to accumulate numerous mutations and to acquire genetic variability^{4,5}, which may drive new subpopulations to appear, leading to intratumour heterogeneity³. Mutations are advantageous for tumour progression if they occur mainly in two types of genes – oncogenes and/or tumour suppressor genes⁶. However, intratumour heterogeneity goes beyond genetics. Non-genetic factors like epigenetic regulation⁷, gene expression stochasticity and tumour microenvironment are also a source of variability⁸. Natural selection and Darwinian evolution can act upon this intratumour heterogeneity, driving cancer progression⁹. Thus, tumour fitness is a consequence of the dynamic interaction between tumour subpopulations¹⁰, and with the cells that compose their tumour microenvironment¹¹.

1.3 Tumour microenvironment

Cancer cells can interact with each other, but they can also recruit a variety of cells to form a complex ecosystem, the tumour microenvironment (TME). The TME differs from cancer to cancer and is mainly composed by fibroblasts, mesenchymal stem cells, adipocytes, endothelial cells, haematopoietic derived cells (both lymphoid – B, T and NKT cells – and myeloid – neutrophils, macrophages and myeloid-derived suppressor cells, MDSCs) and non-cellular components such as the extracellular matrix, ECM^{1,12}. It has been shown that these distinct TME cells may allow tumours to acquire hallmark traits such as sustained growth, metastasis and evade immunity¹³. For example, Quail and colleagues showed that the TME causes resistance to the inhibition of CSF-1R in gliomas¹⁴.

Interestingly, the role of these cells, including immune cells, in tumour progression may vary between cancers and during the tumour progression itself¹³.

Immune cells, as part of either innate or adaptive immunity, may have an anti- or pro-tumour effect in response to cancer cells^{15,16}. Recently, it was shown that innate immune cells are one of the major components of the TME¹⁷. For example, neutrophils and macrophages, as professional phagocytes, exhibit an anti-tumour response by clearing dead and abnormal cells¹⁸. However, in response to specific environmental cues, these immune cells are a major source of angiogenic, epithelial, stromal growth factors and they play a major role in creating an immune suppressive TME¹⁹ that supports neoplastic progression^{13,20,21}.

Neutrophils can recognise cancer cells by distinct mechanisms such as the recognition of damage-associated molecular patterns (DAMPs), neo-antigens or “eat-me signals”. Neutrophil recruitment occurs via proinflammatory signals including hydrogen peroxide, lipid mediators (eg. LTB₄), cytokines (eg. TNF α) and chemokines (eg. CXCL1, CXCL2 and CXCL8²²)²³. However, this recruitment is a multiphase process, where each step is mediated by different cues/processes: forward migration, neutrophil recruitment amplification and neutrophil removal (eg. Macrophage-mediated phagocytosis, apoptosis or reverse migration)^{23,24}. Interestingly, it has been shown that in response to environmental signals such as the expression of TGF β in the TME, neutrophils may acquire a pro-tumour phenotype by promoting angiogenesis and/or metastasis²¹.

Like neutrophils, macrophages in the TME may also have an anti- or a pro-tumour effect. The classical activated M1 macrophages can kill microorganisms and tumour cells and produce different types of pro-inflammatory cytokines (eg. IL-12 and TNF), which are associated with an anti-tumour response. In contrast, the M2 phenotype reduces the inflammatory response and can promote an immunosuppressive TME (eg. secretion of IL-10), which is characteristic of a pro-tumour response²⁵. M2 macrophages do not constitute an uniform population and are subdivided in categories according with their function: M2a, are involved in the T-helper type 2 immune response; M2b are immunoregulatory and secrete large amounts of IL10 and TNF- α ; and M2c are anti-inflammatory and secrete TGF- β and IL-10²⁶. Nevertheless, the three subpopulations are characterised by high production of IL-10 and low production of IL-12²⁷. The TME can polarise both neutrophils and macrophages, promoting a pro-tumour functions versus an anti-tumour phenotype, for example in response to TGF- β ²¹.

The innate immune response requires a coordinated interaction between neutrophils and macrophages, in which they can modulate each other behaviour²⁸. On one hand, the presence of neutrophils can be amplified and sustained either by active neutrophils themselves or by tissue-resident macrophages. On the other hand, differentiation of monocytes into macrophages is stimulated by particles present at neutrophils granules such as cytokines, chemokines and lipids. Furthermore, neutrophils are involved in the activation and recruitment of natural killer (NK) cells, dendritic cells (DCs), and mesenchymal stem cells^{22,23}. NK cells are another crucial component of innate immunity that can recognise and kill cancer cells and thereby reduce tumour growth^{29–31}.

To conclude, the interaction between tumour cells and their microenvironment is a complex and dynamic process in which neutrophils and macrophages are the major players³². Different cues can be found in the TME that can modulate both innate immune cell functions and tumour biology, which may drive neoplastic progression¹³. Therefore, it is fundamental to understand the effect that immune cells have on cancer.

1.4 From immune surveillance to immune escape

Through our lives, billions of cells acquire mutations daily, some of which may drive cells to become cancer cells. However, the immune system is able to recognise and eliminate them before it becomes a clinical apparent disease – a process known as immune surveillance^{33,34}.

In a heterogeneous tumour, different subpopulations may express distinct phenotypic characteristics, like the capacity of evading anti-tumour immunity³. In other words, the capacity of immune cells to recognize and eliminate cancer cells is not equal for the different subclones within a tumour – some are recognized, others are not³. The dual effect of the immune system on tumour progression is described by the tumour immunoediting process^{33,35} that goes hand in hand with Darwinian selection^{13,36}. This process is composed of three phases – elimination, equilibrium and escape³³. The elimination phase requires both innate and adaptive immune systems to recognize a developing cancer and to clear it, avoiding a clinical apparent outcome. It is tightly coordinated and only rare tumour variants may survive this phase. Next, during the equilibrium phase, the adaptive immune system cells sculp the immunogenicity of surviving subclones and prevent tumour cells outgrowth, keeping the residual tumour cells in a functional state of dormancy. It is in this phase that both tumour cell and TME populations can change due to tumour immunoediting, which may drive the progression to the escape phase. In the escape phase, cancer cells that acquired the capacity to evade the immune system emerge as visible tumours: they can circumvent immune recognition (eg. loss of antigens) and/or immune destruction (eg. induction of anti-apoptotic mechanisms). Importantly, tumour cells can promote the development of the escape phase through the production of several immune suppressive molecules, such as PDL-1, CTL4, TGF- β and VEGF³³, generating an immune suppressive TME.

To demonstrate and illustrate the tumour immunoediting process^{37–42}, Schreiber and colleagues performed an experiment in which chemical carcinogens were injected in two groups of mice – one that had a competent immune system (WT) and other with a compromised immune system (Rag^{-/-}). Results showed that more tumours were formed in immunodeficient mice (58%) than in immunocompetent mice (19%), suggesting that an immunocompetent system can prevent tumour formation. Following, subsequently tumours that had grown under the immune selective pressure (tumours formed in immunocompetent mice, “immuno-edited”) and tumours that were grown without the immune selective pressure (tumours formed in immunodeficient mice, “unedited”) were injected into immunocompetent mice (WT). Whereas previous edited tumours could evade the immune system and implant successfully in mice (100% of implantation), unedited tumours were recognised/eliminated by the immune system and cannot successfully implant (50% implantation)^{33,43,44}.

The tumour immunoediting process parallels Darwinian selection, driving cancer progression¹³. As a consequence of this process, tumour immunogenicity should decrease, as they acquire capacity to evade the immune system. These less immunogenic tumours acquired a high capacity to implant in immunocompetent hosts. Thus, the study of tumour implantation may highlight the immune-tumour cell interactions during the immunoediting process that drives cancer progression. Understanding the mechanisms by which immune cells can evade the immune system may uncover new targets to complement ongoing tumour immunotherapeutic approaches.

1.5 Zebrafish as a model to study tumour implantation/rejection

The animal model zebrafish (*Danio rerio*) was recently shown to be a reliable strategy to study tumour implantation/rejection⁴⁵. In fact, xenotransplantation of different human tumour cell lines into zebrafish has shown distinctive implantation efficacy in just 4 days-post injection. These differences

were also observed between cells derived from different stages of cancer progression of the same patient (intra-tumour heterogeneity)⁴⁵. In this assay, tumour cells remained within the zebrafish host between 2-6 days post-fertilisation (dpf), during which the adaptive immune response is not yet established⁴⁶. Thus, this *in vivo* system allows the study of tumour implantation/rejection specifically in response to innate immunity, in which neutrophils and macrophages are the major components.

1.6 Zebrafish immune system

Similar to the immune system in mammals, zebrafish immune response is divided in two subtypes: the innate and the adaptive immune response⁴⁶. The innate immunity is the first line of defence which quickly acts to neutralise a threat (eg. neutrophils, macrophages, dendritic, natural killer (NK) cells and plasma proteins (complement))⁴⁷. When this immune response is overcome, the adaptive immunity is activated. This slower response is more specific and is divided in a humoral response mediated by B lymphocytes and in a cell-mediated immunity mediated by T cells⁴⁸. Haematopoiesis, is the process by which HSC give rise to all differentiated blood cells and the transcription factors and signalling pathways that regulate the formation of hematopoietic stem cells (HSCs) and has been shown to be generally conserved in zebrafish⁴⁹.

The HSCs give rise to two haematopoietic lineages: the myeloid lineage, derived from the common myeloid progenitor (CMP), leading to erythrocytes, granulocytes (eosinophils, basophils and neutrophils) and monocytes (that differentiate in macrophages or dendritic cells); and the lymphoid lineage, which gives rise to lymphocytes (that differentiate in natural killer (NK), B and T cells)⁴⁸.

As all vertebrates, zebrafish haematopoiesis has two waves (Fig. 1.2). The embryonic primitive haematopoiesis leads to the production of myeloid cells and it starts around 11hpf, when haemangioblasts (expressing *Scl*, *lmo2*, *gata2* and *fli1* genes) appear in the lateral mesoderm. Whereas the anterior lateral mesoderm forms the rostral blood island (RBI), which is the major site for myeloid cells (*pu.1*⁺ cells)⁴⁶; the posterior lateral mesoderm becomes the intermediate cell mass (ICM), where

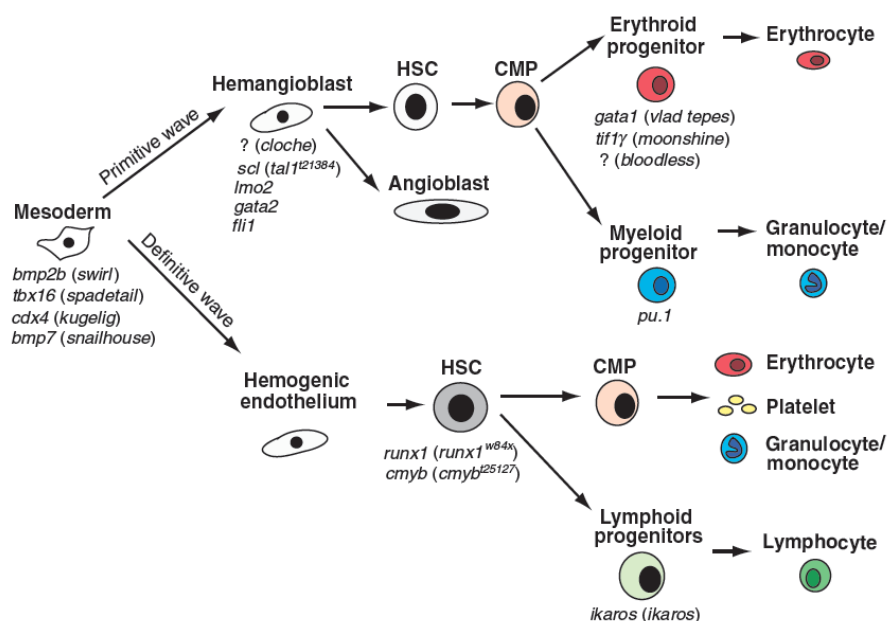


Figure 1.1 **Zebrafish haematopoiesis has two haematopoietic waves.** An illustrative scheme of zebrafish haematopoiesis showing the two haematopoietic waves. Haematopoiesis is the generation of haematopoietic stem cells that drive specific blood lineages with distinct functions. Each step of this process involves the regulation of gene expression, some of which are indicated in the figure. Adapted from ⁵⁰.

primitive erythrocytes appear (*fms*⁺ and *gata1*⁺ cells)⁴⁶. Circulation begins around 24hpf and early myeloid cells (*pu.1*⁺ cells- monocytes and granulocytes, *mpx*⁺ - neutrophils⁴⁶, *mpeg*⁺⁵¹ and *irf8*^{+ 52}- macrophages) migrate to the yolk⁵³. Around this time, the definitive wave of haematopoiesis emerges and HSC (*c-myb*⁺ and *runx1*⁺) arise in the aorta-gonad-mesonephros (AGM)^{46,54}, which will then migrate and colonize the caudal haematopoietic tissue (CHT) at 48hpf to promote erythroid and myeloid cells formation. By 3dpf, HSCs migrate to the thymus where lymphopoiesis begins. Around 4-5 days, haematopoiesis shifts to the kidney marrow, the adult haematopoietic organ in zebrafish^{46,54,55}. T cells are not detectable out of the thymus until 3 weeks post-fertilisation (wpf) and zebrafish are exposed to environmental pathogens for 4 weeks without a functional adaptive immune response⁴⁶. Although zebrafish also present functional NK cells, it is not described in which stage of zebrafish development they appear. Nevertheless, NITR (novel-immune type receptors) share similar structures with mammalian NK receptors and are expressed during embryogenesis. Since adaptive immune system is not yet mature, it is speculated that these NITR receptors may play an important role in innate immunity⁴⁶ or NK cells may appear early. However, it is unknown due to the lack of available markers.

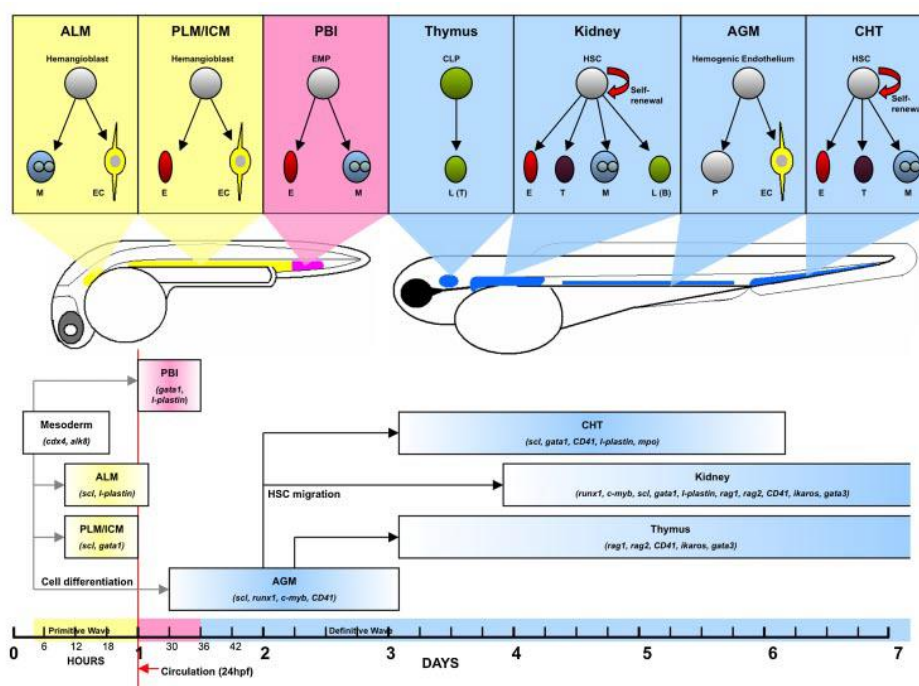


Figure 1.2 Zebrafish haematopoiesis during larvae development is regulated by different transcriptional genes. Zebrafish haematopoiesis takes place in specific sites that change during development. This process occurs through the primitive wave, followed by a transient and a definitive wave. During development, each step is tightly regulated, and the timing of each event is well characterised. Adapted from ⁵⁰.

1.7 Studying tumour-immune cells interactions using the zebrafish model

Previous laboratory results showed that two colorectal cancer (CRC) cell lines derived from the same patient – SW480, derived from the primary tumour and SW620, derived from a lymph-node metastasis (6 months later) – have distinct implantation efficiencies after being xenotransplanted into the zebrafish PVS. SW480 has on average ~30% of implantation success whereas SW620 has ~80%. Surprisingly, SW480 implantation is enhanced either in the presence of SW620 (“MIX”, co-injection of SW480+SW620, 1:1) or after genetically suppression of the myeloid lineage (Pu.1 morpholino injection) (*M. Fuzeta*, master thesis). These results suggest that SW620 may have the capacity to suppress the immune system, facilitating engraftment of SW480. Also, preliminary data uncovered a cooperative interaction between SW480 and SW620, regarding their proliferative capacity and cell death (apoptosis).

The present work is sought to gain insights on to the mechanism that governs rejection/implantations of these SW480/SW620 cell lines. To find the mechanism underlying this process, it is first important to study the intricate interactions that occur between SW480, SW620 and the host immune system, in order to unravel the major players that modulate engraftment efficiency. The main hypothesis that will be addressed in this work is illustrated in figure 1.3. We took advantage of transgenic zebrafish larvae to study the immune cells that compose the tumour microenvironment and that may have a role in implantation/rejection of tumour xenotransplants. As depicted in figure 1.3, this work aims to characterise SW480 and SW620 interactions during tumour implantation/rejection and also to compare the TME of SW480, SW620 and MIX regarding neutrophil and macrophage populations.

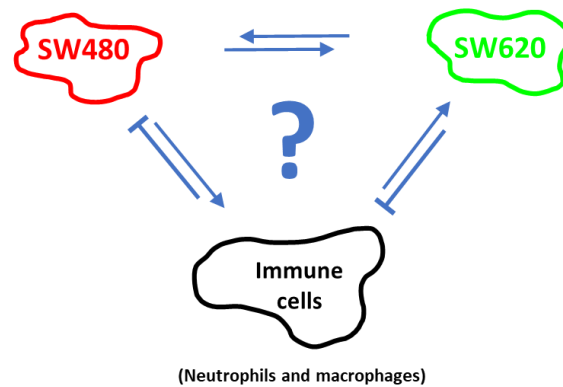


Figure 1.3 **Unravelling the mechanism behind engraftment efficiency.** Illustration of possible mechanisms that may have a role in tumour implantation/rejection. To understand this process, this work will focus on the three main interactions that may be taking place *in vivo*. First, it is important to study the nature of SW480 and SW620 interaction, confirming their proliferative and apoptotic cooperation, which is one likely candidate to improve engraftment rates. Following, the neutrophil and macrophage populations in the TME of SW480 and SW620 will be analysed. It is hypothesised that immune cells have an anti-tumour effect in response to SW480 (tumour rejection) and a pro-tumour effect in response to SW620 (tumour implantation in an immunosuppressive TME). Thus, innate immune cells are potential candidates that may modulate engraftment efficiency.

2. Results

2.1 SW620 prevents SW480 rejection and both cooperate to increase tumour proliferation and survival

In order to further investigate the mechanism behind tumour rejection and engraftment efficacy, we started by repeating previous experiments to establish the experimental set-up and consolidate the preliminary results. Thus, the pair of CRC cell lines, SW480 and SW620, were injected in the perivittelline space (PVS) of zebrafish larvae with 2 days post fertilization (dpf) either alone or mixed in equal proportions (1:1). Results were analysed regarding engraftment, proliferation, apoptosis and total cell numbers of the tumour (Fig.2.1.1).

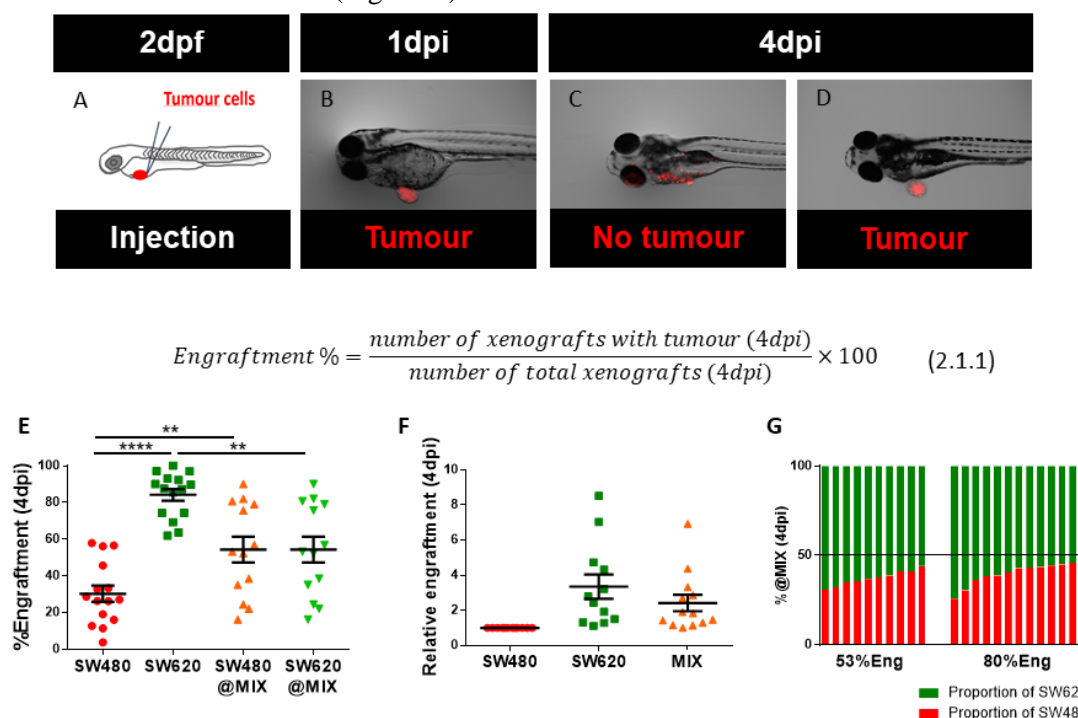


Figure 2.1.1 Engraftment analysis of a pair of human CRC cell lines zebrafish-xenografts. Experimental steps to quantify engraftment rate (A-D). Tumour cells are injected into zebrafish PVS at 2dpf (A). Successfully injected fishes are selected at 1dpi (B) and are left to develop for three more days. At 4dpi, all xenotransplants are scored – no tumour (C) vs tumour (D). Engraftment is calculated with equation 2.1.1. Comparison of the engraftment rate (4 dpi) between SW480 and SW620 cell lines, either injected alone or co-injected. Dots of each group represent independent experiments. Statistical analysis was performed using a paired t test: SW480 vs SW620 ($p < 0.0001$); SW480 vs SW480@MIX ($**p = 0.0025$) and SW620 vs SW620@MIX ($**p = 0.0013$). SW480 ($30.22 \pm 4.430\%$, 15, 1040), SW620 ($84.19 \pm 3.199\%$, 15, 1282) and MIX (54.29 ± 7.085 , 13, 852) (mean \pm SEM, number of independent experiments, number of xenotransplants) (E). To analyse how much SW480 engraftment is increased in the presence of SW620, differences were analysed per experiment. Figure F shows the engraftment of SW480, SW620 and MIX normalised by SW480 engraftment, per experiment. On average, SW620 engraftment is 3.533 ± 0.692 times higher than SW480. Within the MIX (or in other words, in the presence of SW620) SW480, increases its engraftment 2.422 ± 0.468 times. Comparison of SW480|SW620 proportions between one MIX experiment with 53% of engraftment and other with 80% (G).

At 1 day-post injection (dpi), successfully injected tumours were selected to proceed, i.e., all unsuccessfully xenotransplantations were discarded (Fig. 2.1.1.B). At the end of the assay, 4dpi, all xenografts were scored according to tumour presence or absence (Fig. 2.1.1.C-D) and fixed for further analysis. Dead xenotransplants were discarded daily. This work strategy allows the study of engraftment, considered as a percentage of the number of xenotransplants with tumour at 4dpi divided by the total number of xenotransplants at 4dpi (Equation 2.1.1).

The engraftment efficiency of SW480, SW620 and “MIX” independent experiments were analysed (Fig. 2.1.1.E). SW480 presented an engraftment rate of 30.22% which clearly contrasts with 84.19% of SW620. The MIX condition presented an engraftment average of 54.29%. This means that, when co-injected *in vivo*, SW480 cells engraft much more efficiently in the presence of SW620 (from ~30% to 54.29%) while SW620 reduce their engraftment in the presence of SW480. Although the engraftment capacity of SW480 and the MIX is highly variable, between experiments it was consistently observed that SW480 engraftment is enhanced in the presence of SW620 (MIX), with an average increase of 2.42 per experiment (Fig. 2.1.1.F).

Considering that MIX implantation efficacy varies, it can be asked if MIX engraftment is dependent on SW480|SW620 proportion, i.e. MIX experiments with low engraftment would have a higher proportion of SW480 and that MIX experiments with higher engraftment would present a lower proportion of SW480. To address this question, the proportion of SW480|SW620 was compared between one experiment with 53% of engraftment and other with 80% of engraftment. As shown in figure 2.1.1.G, these two MIX experiments with different engraftments present similar proportion of SW480|SW620, suggesting that these proportions (at MIX) do not influence engraftment capacity. However, further experiments to compare engraftment efficiency of these cell lines co-injected at different proportions could complement these observations.

To characterise the total cell numbers, proliferation (mitotic figures) and apoptosis (caspase3 positive cells), an immunofluorescence assay was performed in xenografts at 4dpi and analysed by confocal microscopy (Fig. 2.1.2.A-I). Results show that after 4 days, SW620 total cell number is higher than SW480 either when they are injected alone or mixed (Fig. 2.1.2.J) Thus the proportion of SW620 is higher than SW480 at MIX (Fig.2.1.2.K). As observed in previous results in the laboratory, mitosis and apoptosis quantification also revealed that SW480 proliferation is enhanced in the presence of SW620 (Fig. 2.1.2.L) and SW620 apoptosis decreases in the presence of SW480 (Fig. 2.1.2.M),

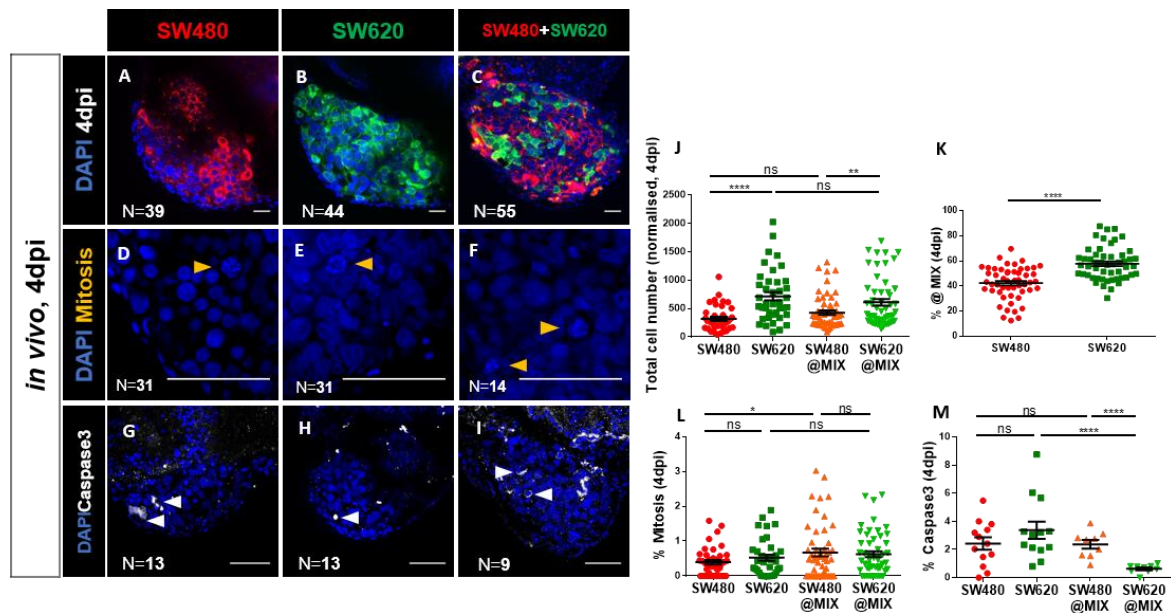


Figure 2.1.2 SW480 proliferation increases in the presence of SW620 and SW620 apoptosis decreases in the presence of SW480 at 4dpi. Images of confocal microscopy showing representative xenografts into zebrafish PVS at 4dpi - SW480 (A, labelled with vibrant CM-DiI, in red), SW620 (B, labelled in DeepRed Cy5, in green) and MIX (C). Nuclei were stained with DAPI (blue). Yellow and white arrowheads indicate mitotic figures (D-F) and apoptotic cells (G-I), respectively. Numbers indicate the xenotransplants analysed. The total cell number of SW480 and SW620 were divided by the factor 2 (normalised). Results are from at least three independent experiments and each dot represents one xenotransplant. Bars represent the mean and the standard error of the mean (mean±SEM). Statistical analysis to compare differences between groups was performed using an unpaired t-test: total cell number (J, ****p<0.0001, **p=0.0073), SW480/SW620 fraction at MIX (K, ****p<0.0001), mitotic index (L, *p=0.0487) and apoptotic index (M, ****p<0.0001) at 4dpi. Scale bars represent 50µm.

suggesting a cooperative interaction between these pair of CRC cells in relation to proliferation and apoptosis.

In summary, this SW480-SW620 interaction is generating four different phenotypes:

- SW480 engraftment increases in the presence of SW620;
- SW620 engraftment decreases in the presence of SW480;
- SW480 proliferation increases in the presence of SW620 and
- SW620 apoptosis decreases in the presence of SW480.

These results highlight the hypothesis that proliferation and apoptosis may be modulating engraftment efficiency, prompting us to explore the nature of these cooperative interactions.

2.2 SW480 and SW620 cooperative interactions seem to be non-tumour-autonomous

The cooperative interaction between SW480 and SW620, regarding proliferation and apoptosis, may be the result of the direct interaction between these cells, exclusively dependent on their intrinsic properties (tumour-autonomous), or in contrast be dependent on the *in vivo* microenvironment (non-tumour-autonomous). Therefore, to discriminate if SW480-SW620 interaction is tumour-autonomous or non-tumour-autonomous, an *in vitro* assay was performed (Fig 2.2) to discard the *in vivo*

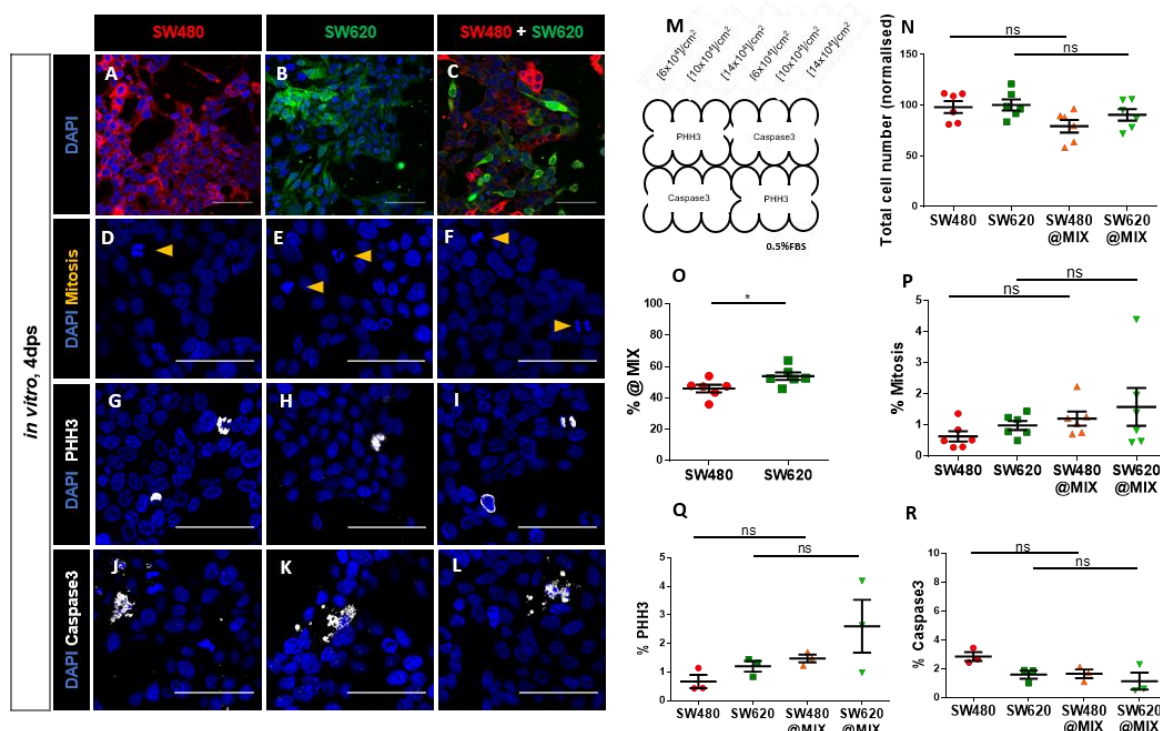


Figure 2.2 SW480 and SW620 do not seem to interact *in vitro*. Confocal representative images of SW480 (A, labelled with vibrant CM-DiI, in red) and SW620 (B, labelled in DeepRed, in green) either seeded alone or co-cultured (C) at 4 days-post seeding (dps). Representative images of mitotic figures (D-F, yellow arrowheads). Whole-mount immunofluorescent staining at 4dps for Phospho Histone H3 (PHH3) (G-I, white) and Caspase3 (J-L, white). Nuclei staining with DAPI (blue). Cells were seeded with 0,5%FBS and results are referent to a cell density of 14x10⁴ cells/cm². Experimental layout of the *in vitro* experiment in a 24-well plate. Each condition (SW480, SW620 or MIX) was seeded in a different plate with 0,5% FBS. Different cell densities were tested, however the results are only referent to the higher concentration (14x10⁴ cells/cm²). Immune antibodies were organised as described to avoid external factors bias (M, P3-PHH3 and C3-Caspase3). Quantification of total cell number (N), percentage of SW480 and SW620 at MIX (O), percentage of mitotic figures (P) percentage of PHH3 positive cells (Q) and caspase3 activated cells (R) at 4dps. The total cell number of SW480 and SW620 were divided by the factor 2 (normalised). Statistical analysis was performed using an unpaired t-test student. Scale bars represent 50µm. Each dot represents the average of the quantification of 6 tile-scan images (2x3) per coverslip. P-value: ns>0,05, *≤0,05, **≤0,01, ***≤0,001, ****≤0,0001.

environment. In other words, if the interactions are only dependent on their intrinsic properties we expect to observe the same cooperative interaction regarding proliferation and apoptosis also *in vitro*.

In this experiment, we compared the behaviour of the mono-cultures of SW480 (Fig. 2.2.A) and SW620 (Fig. 2.2.B) with the co-culture of both cell lines (Fig. 2.2.C). Each condition – SW480, SW620 and MIX – was cultured in 0.5% FBS, and after testing different cell densities to assure cell-contact, 14×10^4 cell density was chosen for analysis (Fig. 2.2.M). Different parameters were analysed such as: total cell number (Fig. 2.2.N), the percentage of SW480 and SW620 when co-cultured (O), the mitotic index (Fig. 2.2.P) and the percentage of PHH3 positive cells (Fig. 2.2.Q) as a proxy for proliferation capacity and the percentage of Caspase3 positive cells (Fig. 2.2.R) as readout for apoptosis.

Our results show no statistically significant differences when comparing mono vs co-culture, suggesting that SW480 and SW620 cooperative interaction is non-tumour-autonomous, occurring only in an *in vivo* environment.

2.3 Tumour clearance over time

The results above suggest that SW480-SW620 interactions may be mediated by their TMEs. Therefore, the next step was to further characterise these phenotypes *in vivo*. First, the dynamic interactions of engraftment/rejection were analysed along time, by quantifying engraftment at consecutive time-points (2, 3 and 4dpi). The starting point was considered at 1dpi upon tumour screening, in which all xenografts of the 3 conditions exhibited tumour (engraftment=100%). The figure 2.3 shows the average of engraftment for three independent experiments of SW480 (red), SW620 (green) and MIX (orange). Since the first time-point at 2dpi, engraftment rates of the three conditions start diverging (z-test, $p < 0.001$). SW480 shows a steep slope between 1-3dpi. MIX decline is not as strong as SW480 and seems similar between time-points. SW620 engraftment between time-points has little variation.

Overall, these results indicate that the reduction of engraftment is a dynamic and continuous process but also highlight the intermediate engraftment efficiency of MIX, suggesting the possibility of conflicting signals that modulate engraftment.

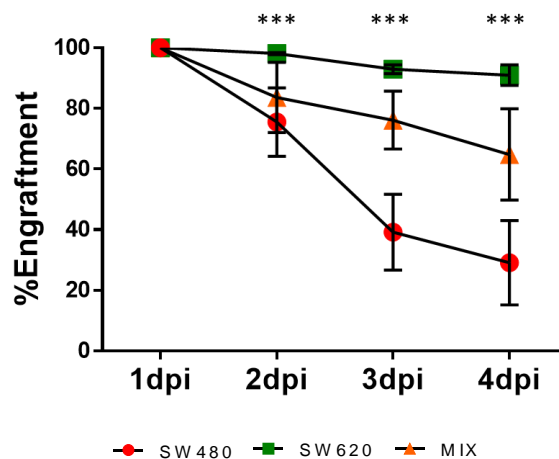


Figure 2.3 Tumour clearance is a continuous process and differs between tumour cell lines derived from the same patient. Engraftment rate was measured at consecutive days during the experiment: 2, 3 and 4dpi. Graph represents a time-course clearance of SW480, SW620 and MIX of three independent experiments ($n \approx 200$ -300 xenotransplants per condition). The error bars represent the standard error of the mean (SEM). Statistical analysis was performed using a z-test to compare SW480 vs SW620, SW480 vs MIX and MIX vs SW620 engraftment rate at 2dpi, 3dpi and 4dpi. All comparisons were significant (**p-value <0.001).

2.4 SW480 and SW620 present different and dynamic behaviours *in vivo* since the first 24hours

This time-course of tumour behaviour also suggests that, by analysing the *in vivo* results only at 4dpi we are looking at engrafted tumours (within the time-window of our assay) and thus we are analysing the net result. Therefore, to understand the differences behind engraftment and rejection we need to step back in time and analyse an earlier time-point when rejection is taking place, comprising both tumours that will engraft and tumours that will be rejected (Fig. 2.4.1). Additionally, the direct comparison between data from two engraftment time-points illustrates well the dynamics that occur during this process (Fig. 2.4.2). Since at 48hpi engraftment differences are already significant (Fig. 2.3), xenografts were analysed at the previous time-point (1dpi) (Fig. 2.4.A-I), to unravel the first selective steps of implantation/rejection.

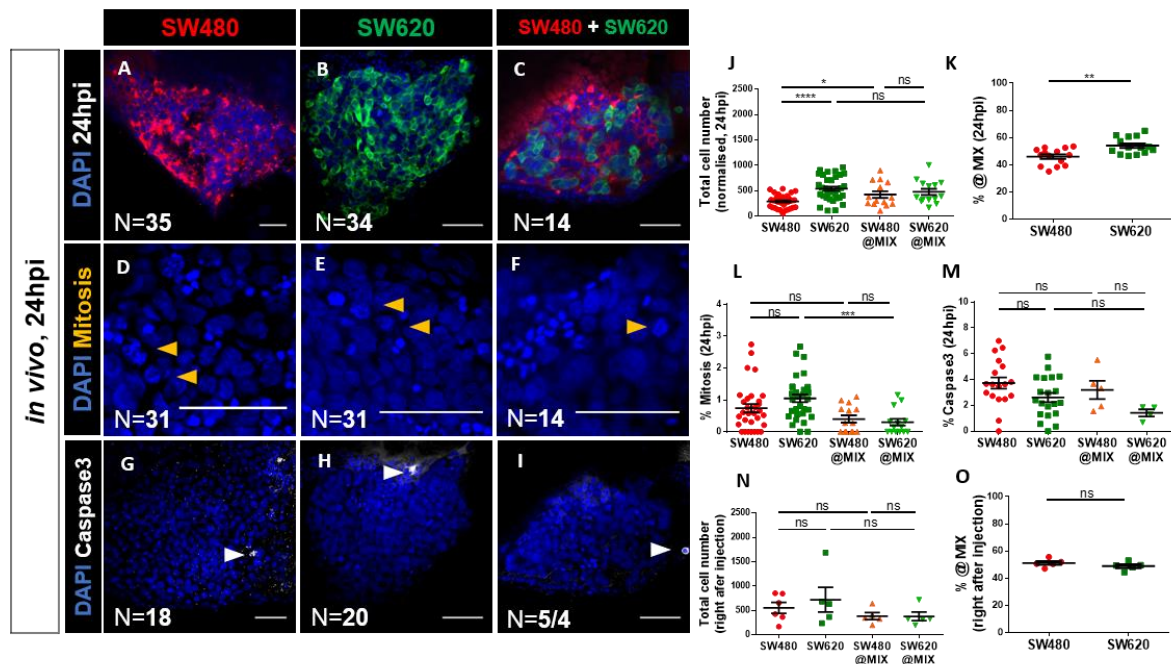


Figure 2.4.1 SW480 and SW620 present different behaviours after 24hours *in vivo*. SW480 (A, labelled with vibrant CM-DiI, in red), SW620 (B, labelled in DeepRed Cy5, in green) and MIX (C) tumours into PVS at 24hpi. Yellow arrowheads illustrate mitotic figures (D-F) and white arrowheads show Caspase3 activated cells (G-I), nuclei staining with DAPI. Quantification of total cell number (J, **** $p < 0.0001$, * $p = 0.0137$), SW480 and SW620 proportion at MIX (K, $p = 0.0017$), mitotic index (L, *** $p = 0.0004$) and percentage of apoptotic cells (M) at 24hpi. Results are from at least three independent experiments. The number of xenografts analysed are indicated in the representative images. Total cell number (N) and SW480/SW620 proportion at MIX (O) right after injection showing that equal numbers of the different cell lines are being injected, either alone or mixed. The total cell number of SW480 and SW620 were divided by the factor 2 (normalised). Each dot represents one xenotransplant as follow: SW480, $n = 6$; SW620, $n = 5$; MIX, $n = 5$. In each graph, is represented the mean and the standard error of the mean (mean \pm SEM). Scale bars represent 50 μ m. P-value: ns > 0.05 , * ≤ 0.05 , ** ≤ 0.01 , *** ≤ 0.001 ,

Following the previous analysis rational, different cell traits such as total cell number (Fig. 2.4.1.J), SW480/SW620 fraction at MIX (Fig. 2.4.1.K.), mitotic figures (Fig. 2.4.1.L) and apoptosis (Fig. 2.4.1.M) were analysed by confocal microscopy. Strikingly, after 24 hours *in vivo*, we already observe different behaviours between mono or polyclonal xenografts (MIX).

However, if we compare the number of SW480 tumour cells in mono vs polyclonal xenografts, we observe that the number of SW480 cells is higher in the presence of SW620 (Fig. 2.4.1.J), suggesting that SW620 is already having a positive impact on SW480. In contrast, the proliferative capacity of

SW620 decreases in the presence of SW480 (Fig. 2.4.1.L), suggesting that SW480 may have a negative effect on SW620.

In summary, in the MIX xenografts, proliferation and engraftment go hand in hand ie, SW480 cells increase proliferation and engraftment whereas SW620 cells decrease proliferation and engraftment. These results suggest that proliferation might contribute to engraftment. If this hypothesis is correct, we would expect that:

1. SW620 would have a higher proliferation rate than SW480 at 1dpi;
2. In the MIX at 1dpi, SW480 increased proliferation in relation to SW480 alone (SW480 engraftment improves at MIX);
3. In the MIX at 1dpi, SW620 decreased proliferation in relation to SW620 alone (SW620 engraftment reduces at MIX) and
4. SW480 xenografts would show a proliferative increase from 1 (tumours that will engraft + be rejected) to 4dpi (engrafted tumours).

Results show that the different conditions have the same proliferative capacity at 1dpi with the exception of SW620 that presents less proliferation in the MIX (Fig. 2.4.1.L). Therefore, we can reject hypothesis 1 and 2 but not hypothesis 3. Hypothesis 4 is also rejected because SW480 proliferation decreases along time (Fig. 2.4.2.A). These results seem to suggest that maybe proliferation is required during SW620 engraftment. So, if this is true, it is expected that SW620 proliferative capacity does not change or increase along time. However, results show that SW620 proliferative capacity reduces along time (Fig. 2.4.2.A), suggesting that proliferation does not play a major role on engraftment.

Another hypothesis could be that rejection/engraftment is modulated by apoptosis, ie, a decrease in apoptosis would correlate with an increase of engraftment and vice versa. If this is the case, then we expect that:

1. SW480 cells would have a higher level of apoptosis than SW620 at 1dpi,
2. In MIX at 1dpi, SW480 reduced apoptosis in relation to SW480 alone (SW480 engraftment improves at MIX);
3. In MIX at 1dpi, SW620 increased its apoptosis in relation to SW620 alone (SW620 engraftment reduces at MIX) and
4. SW480 would reduce apoptosis from 1 (tumours that will engraft + be rejected) to 4dpi (engrafted tumours).

However, our results show that only premise 4 is significant (Fig. 2.4.2.B). We can reject hypothesis 1, 2 and 3 since at 1dpi there is no apoptotic differences between conditions (Fig. 2.4.1.M). More importantly, and contrary to what was expected, we observe that SW620 at MIX has less apoptosis and presents lower engraftment than SW620 alone at 4dpi. These results suggest that tumour rejection is independent of cell death.

All in all, these results suggest that neither proliferation nor apoptosis are behind engraftment differences. Interestingly, the previous cooperative interaction between SW480 and SW620 is not yet observed at 1dpi: SW480 proliferation is not increased in the presence of SW620 (Fig. 2.4.1.L) and SW620 apoptosis is not decreased in the presence of SW480, although our number of samples for the apoptotic index is not as robust and therefore these experiments should be repeated (Fig. 2.4.1.M).

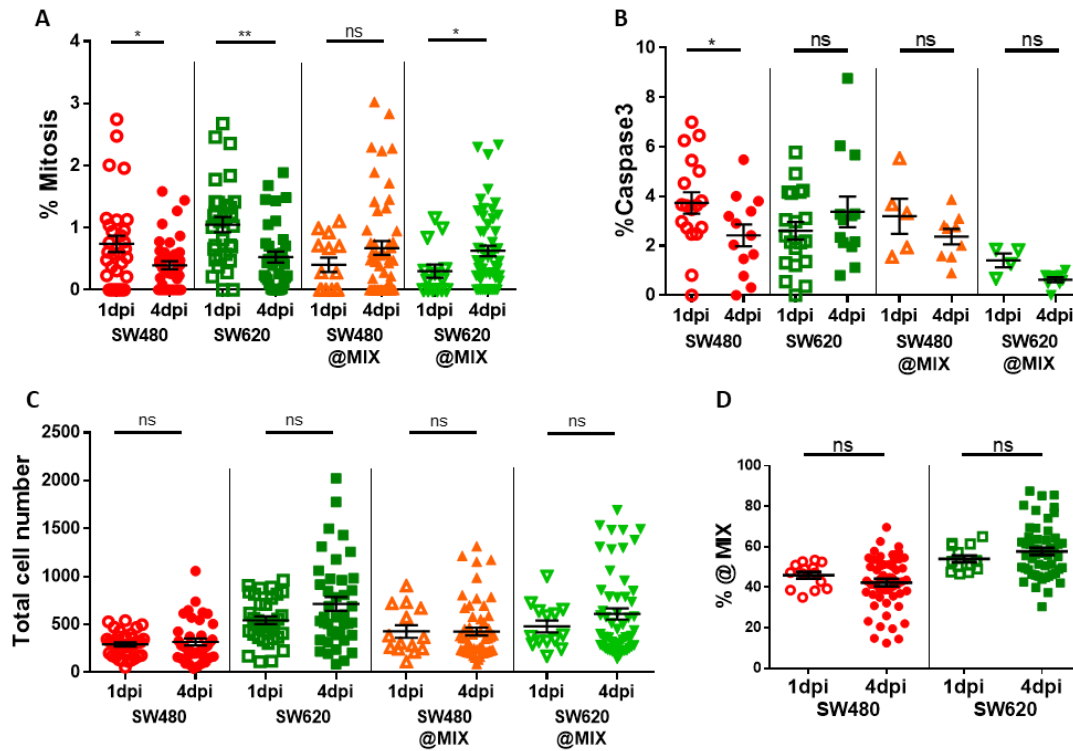


Figure 2.4.2 **The *in vivo* SW480 and SW620 behaviour along time is a dynamic process.** Comparison between 1dpi and 4dpi phenotypes of SW480 and SW620, either alone or co-injected, regarding the mitotic percentage (A, SW480 * $p=0.0321$, SW620 ** $p=0.0012$, SW620@MIX * $p=0.0411$), apoptotic index (B, * $p=0.0479$), total cell number (C) and SW480/SW620 proportion at MIX (D). Statistical analysis was performed using an unpaired t-test. Each dot represents one xenograft.

Importantly, at 24hpi in MIX xenografts we observed that the SW480|SW620 fraction is no longer 1:1, and that SW620 is becoming dominant, with a higher number of SW620 cells per xenograft (Fig. 2.4.1.K). Also, when we compare SW480 and SW620 monoclonal xenografts we already observe that SW620 tumours have more cells (Fig. 2.4.1.J). In addition, these xenografts total cell number and fraction at MIX do not alter over time (Fig 2.4.2.C-D). This raised the question whether we were having a technical problem and were injecting un-equal proportions of SW480/SW620 cells. Thus, to discard this, we analysed xenografts right after injection. However, our results show no difference in SW480/SW620 total cell number and/or fraction at MIX after injection (Fig. 2.4.1.N-O), showing that in the first 24h *in vivo* interactions are already occurring and accounting for the dominance of SW620 after 24hpi.

2.5 SW480 recruits higher number of neutrophils than SW620

In summary, we showed that engraftment/rejection is a highly dynamic process and that SW480/SW620 cells cooperate *in vivo* regarding proliferation and apoptosis. However, this cooperative behaviour cannot fully explain the engraftment/rejection phenotypes observed. Since SW480 engraftment is enhanced when the innate immune system is suppressed, the innate immune system is our main candidate to modulate engraftment/rejection profiles. To understand the interaction between these pair of CRC cells and the innate immune response, we started by characterising the major myeloid players, namely neutrophils and macrophages, in the TME of the SW480, SW620 and MIX xenografts.

To characterise the neutrophil populations in the different TMEs, these three conditions were injected into Tg(mpx:GFP) zebrafish line with GFP-labelled mpx⁺ cells (a marker for neutrophils myeloperoxidase). At 2 and 4dpi, xenografts were imaged by confocal microscopy and neutrophils present at the TME were quantified. Figure 2.5.A-C shows the neutrophil populations (mpx⁺ cells, false white, indicated by yellow arrowheads) present at SW480, SW620 and MIX TMEs. For each xenograft, the percentage of neutrophils was analysed by the ratio of the number of neutrophils (Fig. 2.5.D-E) divided by the total number of tumour cells (hereafter referred as % mpx). At 1 and 4dpi, our results clearly demonstrate that SW480 primary cells are able to recruit more neutrophils to the TME than SW620 (Fig.2.5.F-G). Interestingly, MIX (SW480+SW620) xenografts recruit intermediate numbers of neutrophils, suggesting again the presence of competing signals, ones to recruit neutrophils and others to evade detection and immune suppression.

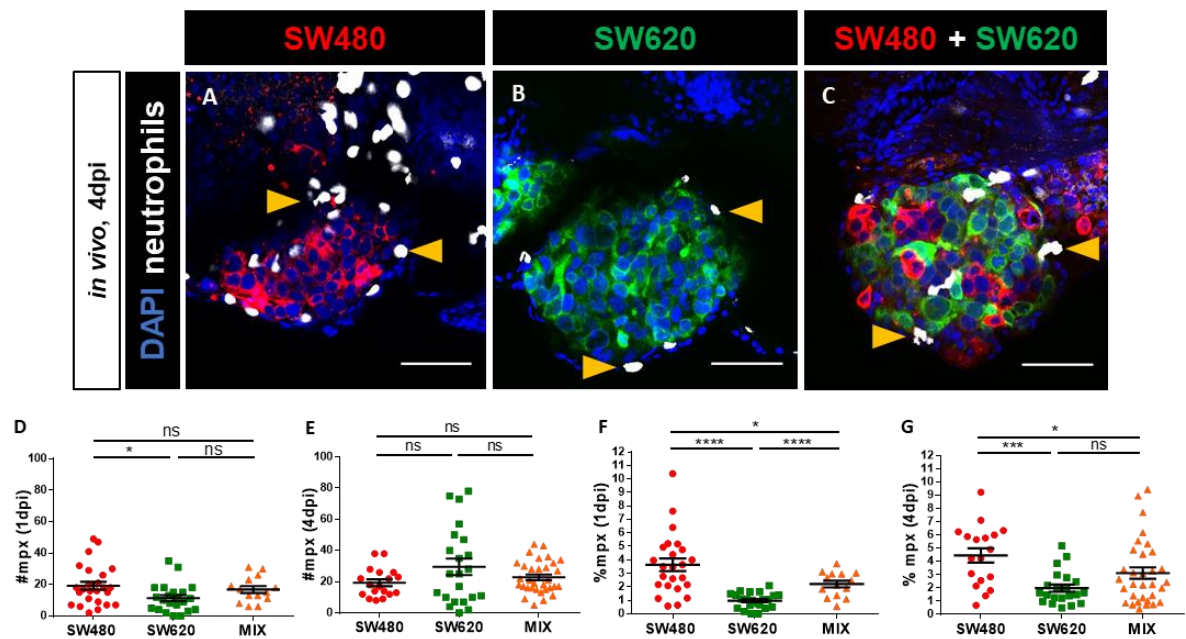


Figure 2.5 Neutrophil populations are higher at SW480 TME. Confocal images represent SW480 (A, labelled with vibrant CM-DiI, in red), SW620 (B, labelled in Cy5, in green) and MIX (C, SW480 + SW620) tumours in mpx:GFP zebrafish transgenic line at 4dpi. Absolute number of neutrophils at 1dpi (D, * $p=0.0204$) and 4dpi (E) were normalised by total cell number per xenograft. Percentage of neutrophils per tumour cell at the TME of SW480 (3.636 ± 0.4686), SW620 (0.9751 ± 0.1235), MIX (2.207 ± 0.2487) at 1dpi (F, **** $P < 0.0001$, * $p=0.0332$) and SW480 (4.457 ± 0.5373), SW620 (1.125 ± 0.4277), MIX (3.125 ± 0.4277) at 4dpi (G, *** $p=0.0001$, * $p=0.0393$). Each dot represents one xenograft from at least three independent experiments. The number of neutrophils analysed for 1 and 4dpi are as follows: 1dpi (SW480, $n=24$; SW620, $n=22$; MIX, $n=14$); 4dpi (SW480, $n=18$; SW620, $n=21$; MIX, $n=32$). Statistical analysis was performed using an unpaired t-test. Arrowheads indicate neutrophils (false white). Scale bar represent 50 μ m. P-value: ns>0,05, * $\leq 0,05$, ** $\leq 0,01$, *** $\leq 0,001$, **** $\leq 0,0001$.

2.6 The number of neutrophils in the TME does not correlate with tumour rejection

Our results showed that SW480 xenografts at 1dpi (some will engraft, and others will be rejected) have a variable percentage of neutrophils per tumour cells (some tumours have low neutrophils and others have high neutrophils) and that SW620 xenografts at 1dpi (the majority of each engraft) have a low percentage of neutrophils. Thus, we can hypothesised that SW480 xenografts with more neutrophils will be rejected, while the ones with fewer neutrophils will engraft. If this stands, a decrease in SW480 TME neutrophils between 1 and 4dpi is expected.

However, the percentage of neutrophils in the TME of SW480 does not change between these two time-points. In other words, the neutrophil population at the TME of xenotransplants that will engraft/be rejected (SW480 at 1dpi) presents no quantitative differences in relation to the TME of

engrafted xenotransplants (SW480 at 4dpi). Despite the clear differences between SW480 and SW620 it seems that the number of neutrophils in the TME does not have an impact on tumour rejection (Fig. 2.6).

In addition, the MIX and the SW620 TMEs become more similar with each other regarding the percentage of neutrophils at 4dpi (Fig. 2.5.G), suggesting that either SW620 or the MIX TME dynamics are changing. Surprisingly, we observed an increase in the percentage of neutrophils in the SW620 TME over time, raising the possibility that neutrophils may contribute to engraftment efficiency.

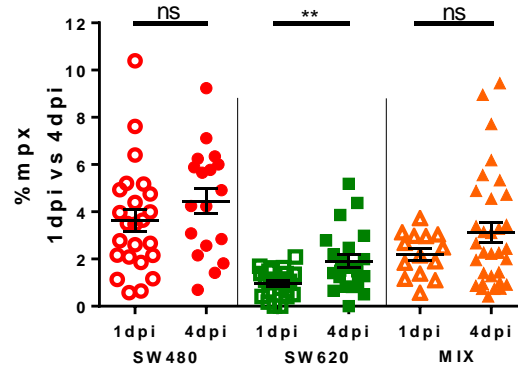


Figure 2.6 **SW620 TME neutrophil populations increase during tumour selection but it is always lower than SW480 TME neutrophil populations.** Comparison of neutrophil percentage at the TME between an early (1dpi) and late (4dpi) time-points. Neutrophil quantification was normalised by the total cell number, per xenograft. Statistical analysis was performed using an unpaired t-test: SW620, ** $p=0.0037$.

2.7 Two distinct mechanisms of tumour cells-neutrophils interaction

Given that the percentage of neutrophils is a ratio between the number of neutrophils and the total tumour cells, it can be asked whether neutrophil number is dependent on the cell number. To elucidate this question, the number of neutrophils and tumour cells per xenograft (Fig. 2.7.A-C) were plotted in correlation graphs (Fig. 2.7.A'-C') and studied by linear regression analysis. The underlined hypothesis is that, if the number of neutrophils is dependent on the number of tumour cells, the linear regression should be different from zero. Therefore, a positive decline would mean that the number of neutrophils are positively correlated with the total cell number, and a negative decline would mean an

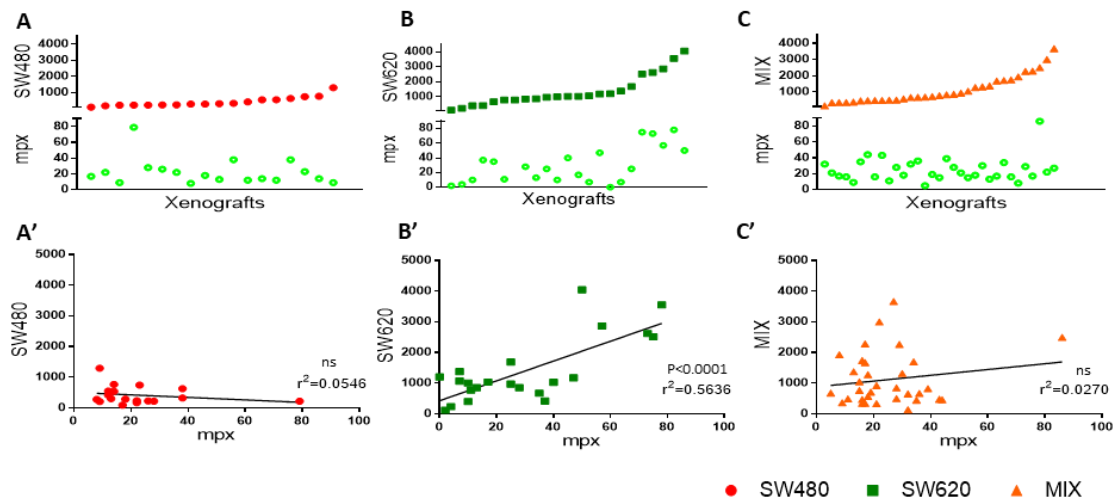


Figure 2.7 **Correlative analysis of neutrophils vs total tumour cells.** Graphs (A, SW480, red dots; B, SW620, green squares; C, MIX, orange triangles) showing the number of neutrophils (A-C, green circles) and tumour cells per xenograft (each column represent one xenograft). Graphs are plotted by total cell number ascending order. In correlation graphs (A', SW480; B', SW620, $p < 0.0001$; C', MIX) each dot represents one xenograft, Y-axis indicates tumour total cell number and X-axis indicates neutrophil absolute numbers. A linear regression and the respective r^2 are represented for each condition. The linear regression slope is significantly different from zero ($p < 0.0001$) in relation to SW620 xenografts.

inverse correlation. Results show a linear regression not different from zero regarding SW480 and MIX TMEs, suggesting that the number of neutrophils is independent on the number of tumour cells (Fig. 2.7.A' and C'). By contrast, in SW620 xenografts (Fig. 2.7.B'), the linear regression slope is significantly different from zero ($p < 0.0001$) and presents a positive slope, suggesting that the number of neutrophils is dependent on the number of SW620 tumour cells.

These results strengthen the idea that neutrophils interact differently with SW480 or SW620. It also suggests a dual mechanism of tumour-neutrophil interaction – one dependent (SW620) and another independent (SW480) on the number of tumour cells. Highlighting distinct tumour cell-host interactions between subclonal populations. Whereas one mechanism is associated with one tumour cell line that is usually rejected from the host (SW480), the other mechanism is associated with one that can engraft efficiently (SW620).

2.8 Characterization of macrophage populations in TME

Neutrophils are not the only players in the TME and they can interact with other surrounding cells. The innate immune response is known to be a result, among others, of a dynamic crosstalk between neutrophils and macrophages. Thus, to understand these interactions in response to tumour implantation/rejection, it is essential to characterise the macrophage populations in the TME. For that, SW480, SW620 and MIX tumour cells were injected into Tg(mpeg:mCherry tnfa:GFP) zebrafish line⁵⁶. This transgenic line allows the identification of macrophages in red (mpeg:mCherry), tnfa⁺ cells in green (tnfa:GFP) and macrophages expressing tnfa in yellow (Fig. 2.8.A-A'''). Mpeg is a well-known marker for macrophages and tumour necrosis factor alpha (tnfa) is a cytokine mainly produced by macrophages and induced in the inflammatory process⁵⁶. At 1 and 4dpi, xenografts were imaged by confocal microscopy and both macrophage and tnfa⁺ cells present at SW620 TME were quantified (Fig. 2.8.B-D). However, this transgenic line is not so strong and reliable as the Tg(mpx:GFP) line and therefore we could only obtain for now, reliable results regarding SW620 xenografts.

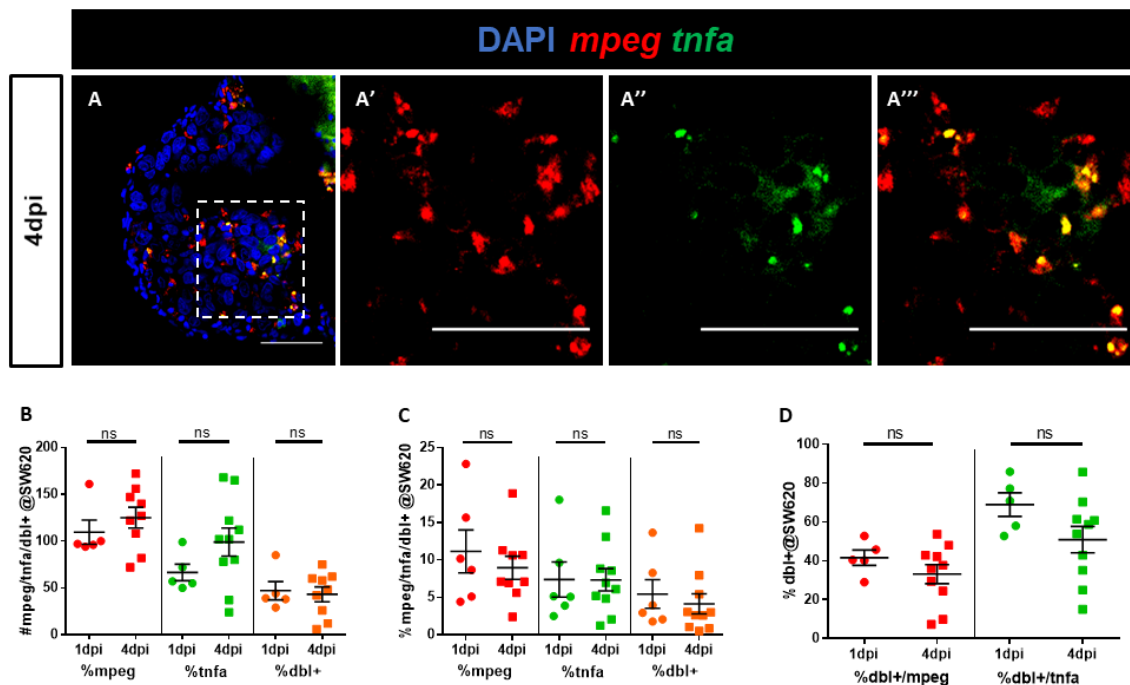


Figure 2.8 SW620 TME macrophage populations over time. Confocal images of a SW620 tumour injected into the PVS of a Tg(mpeg:mCherry tnfa:GFP) zebrafish illustrating the presence of macrophages at the TME (A). Macrophages, mpeg⁺ cells (A', red), can colocalize with tnfa⁺ cells (A'', green) allowing the identification of macrophages expressing tnfa (A''', yellow). The absolute number of innate immune cells at SW620 TME (B) and the respective percentage (C) were compared between 1 and 4dpi. Proportion of macrophage and tnfa cells double positive cells (dbl+) at 1 and 4dpi (D). Each dot represents one SW620 xenograft (n=5 at 1dpi and n=10 at 4dpi).

The number of macrophages (mpeg⁺), tnfa⁺ cells and double positive cells (dbl⁺) was quantified (Fig. 2.8.B). The percentage of these immune cells per SW620 xenograft shows no alterations along time (1 vs 4dpi) (Fig. 2.8.C). However, it is very clear that in the SW620 TME there is a higher abundance of macrophages (~10%) when compared to neutrophils (~1%). Interestingly, ~40% of the population of macrophages is expressing tnfa (Fig. 2.8.D), suggesting the presence of at least 2 different populations of macrophages in the TME, possibly 2 different polarization states. Figure 2.8.D also suggests the presence of other immune cells (non-macrophages) expressing tnfa at SW620 TME. Since we could not characterize the SW480 and MIX xenografts TME, in terms of macrophage populations, we cannot infer more from these results.

2.9 Modulation of zebrafish larvae innate immune system

To decipher the role of neutrophils and macrophages in tumour implantation/rejection, a functional assay is mandatory. Besides genetic manipulation, another strategy to modulate immune cells relies on the application of drugs with an immunosuppressive effect. Interestingly, most chemotherapeutic drugs are known to induce immunosuppression in some patients. In fact, preliminary laboratory results showed that SW480 engraftment increases upon FOLFOX (combination of 5-Fluororacil, oxaliplatin and Folinic acid) chemotherapy treatment. This led to the hypothesis that the increase of SW480 engraftment was due to the immunosuppression caused by FOLFOX treatment. Another pharmaceutical component used to immunosuppression is Tacrolimus, a drug commonly used upon organ transplantation procedures to increase transplant efficiency. So far, the effect of these drugs on innate immunity is not well understood, it is thought that these drugs could reduce the overall numbers of myeloid cells in the host. Therefore, to understand the immunosuppressive effect of FOLFOX and Tacrolimus on the innate immune cells, 2dpf zebrafish transgenic larvae, with neutrophils and macrophage fluorescent-labelled, were submitted to 3 days of treatment. The number of myeloid cells was quantified by flow cytometry. Tg(mpx:GFP) and Tg(mpeg:mCherry tnfa:GFP) zebrafish larvae were randomly distributed between treatment groups (control, FOLFOX and Tacrolimus) and 50

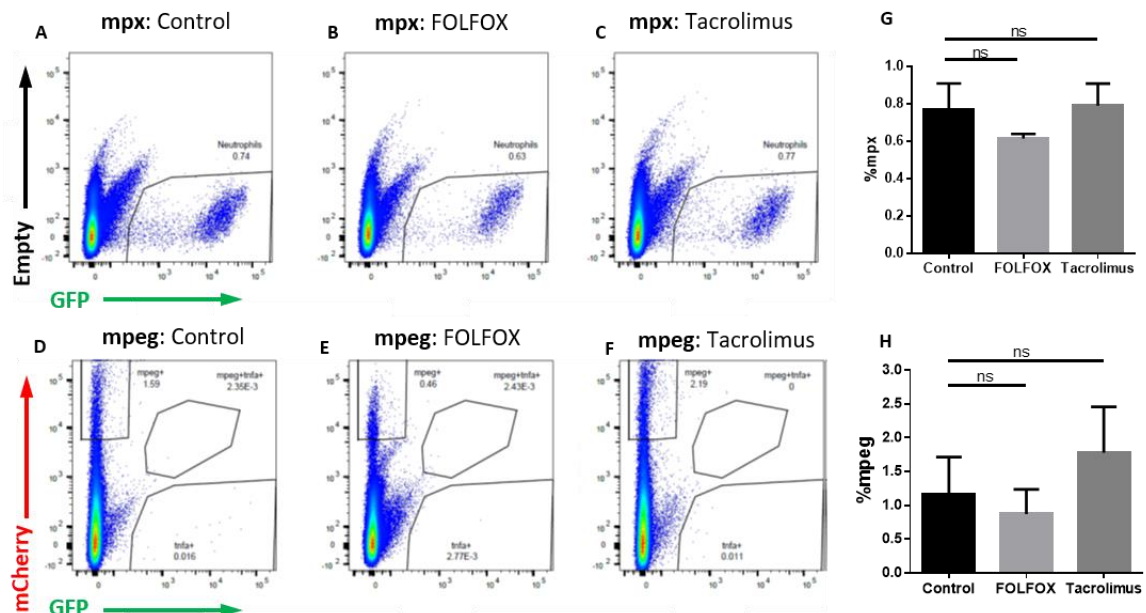


Figure 2.9 Quantification of zebrafish innate immune populations by flow cytometry. Graphed data of representative flow cytometry quantification of neutrophils (mpx:GFP) (A-C) and macrophages (mCherry:mpeg tnfa:GFP) (D-F) upon treatments. Bar graphs show the percentage of neutrophils (G) and macrophages (H) between a non-treated group as a control, a group treated with FOLFOX and a group treated with Tacrolimus. Each group contained 50 zebrafish larvae at 6dpf and 3 days-post treatment (3dpt). Statistical analysis was performed using a paired non-parametric Wilcoxon test. Results are expressed in $AVG \pm SEM$.

larvae of each group (at 6dpf) were sacrificed and prepared to be analysed through flow cytometry (protocol in methods). Then, the percentage of neutrophils (Fig. 2.9.A-C) or macrophages (Fig 2.9.D-F) within each group – control, FOLFOX and Tacrolimus – was quantified. Overall, we did not observe a significant difference in the number of myeloid cells upon treatments after the analysis of 3 independent experiments (Fig. 2.9.G-H). The control groups presented high variability between experiments, and it could be the main explanation for the non-significant differences. This approach should be repeated with increased number of samples per condition, preferentially only considering positive zebrafish transgenic, and with more independent experiments.

Flow cytometry quantification was also tested as one new approach to analyse myeloid populations once this technique can avoid human error and overcome colour limitation, allowing the simultaneous analysis of different parameters. However, it cannot fully replace the previous technique since it loses spatial information. The protocol could also be improved in order to decrease the variability observed. It can be questioned if this approach is advantageous to TME cells quantification, when compared with confocal microscopy. This protocol should be optimised for further FACS and subsequent qPCR analysis.

3. Discussion

The cancer immunoediting concept describes the dual effect of immune cells on cancer development³³. Within a heterogeneous tumour, some subclonal populations may be less recognized than others³. Therefore, when immune cells “clear” a heterogeneous tumour, the less immunogenic subpopulations can remain in the host, leading to the progression of a low immunogenic cancer and further distant metastasis⁵⁷. It has been shown that after going through a tumour “immunoediting” process, the implantation capacity of tumour cells increases³³ in immunocompetent hosts, implying that the tumour implantation capacity is a proxy of the immunogenic state of the cells.

Preliminary data of our laboratory showed that a pair of human CRC cell lines derived from the same patient have contrasting capacities to implant in the zebrafish model. Whereas SW480, derived from a primary tumour, engraft poorly, SW620, derived from a subsequent metastasis, can implant successfully. Surprisingly, the engraftment of SW480 increases in the presence of SW620 and these cells, when co-injected, establish an *in vivo* cooperative interaction regarding apoptosis and proliferative capacity. An increase in SW480 engraftment capacity when the innate immune system has been suppressed was also observed. On the one hand, the results suggest that apoptosis and proliferation capacity could have a role in engraftment, on the other hand these results prompt the hypothesis that SW620 may have an immunomodulatory capacity to change TME on behalf of engraftment efficiency.

The goal of this work was to first consolidate the preliminary data and then to further study the interactions between these cells with the host innate immune cells in their TME. These will allow new and more detailed insights of the mechanism behind engraftment/rejection. Confirming the previous data, we observed 2 major phenotypes when both clones are mixed *in vivo*:

1. The cooperative effect that promotes SW480 proliferation and decrease of SW620 apoptosis.
2. Engraftment phenotype: increase of SW480 and decrease of SW620 implantations.

In order to test whether the cooperative effect is due to tumour-autonomous or non-tumour autonomous interactions, proliferation and apoptosis were analysed *in vitro*, comparing mono- and a co-culture of these cells. Results showed no statistical difference between mono and poly-clonal cultures, suggesting that cells do not engage interactions *in vitro* (Fig. 2.2), and the observed *in vivo* cooperation may be host-dependent. Considering that we only performed one independent experiment and that SW480 proliferation tends to increase in the presence of SW620, this experiment should be repeated to confirm the result obtained. Nevertheless, these results are in accordance with previous laboratory results *in vitro*. Therefore, we focused on the *in vivo* interactions and started by doing a time-course analysis of engraftment. This analysis along time revealed that rejection is a dynamic continuous process, starting as soon as 24h post injection/scoring (Fig.2.3).

This analysis prompts us to step back and analyse a time-point where rejection is actively taking place (1dpi). By doing this, we can analyse a mixture of xenografts that will implant while others will be rejected. Interestingly, the cooperative behaviour observed at 4dpi is not yet established at 1dpi and contrastingly, SW620 proliferation is impaired in the presence of SW480, suggesting that these interactions are highly dynamic. Moreover, comparative analysis of proliferation and apoptosis (1 vs 4dpi) suggest that neither proliferation nor apoptosis can explain engraftment differences. Nevertheless, SW480 tumours have already less cells than SW620 xenotransplants at 1dpi. To understand if total cell number differences at 1dpi are due to active selection, or just a technical caveat, xenografts were fixed right after injection. Results confirmed that all conditions were injected in equal proportions, suggesting a clearance in SW480 total cell numbers within the first 24hpi. However, the tumour total cell number does not change between 1 and 4dpi (Fig.2.4.2.C). This data suggests the existence of two different mechanisms, one occurring during the first 24hpi that decreases total tumour cells (eg, clearance of the

more immunogenic cells), and another that leads to whole tumour implantation/rejection without impacting in the total cell number.

Overall, these results point to a possible role on tumour-host interactions for engraftment/rejection process. Therefore, we decided to characterize the TME. SW480 TME has a higher percentage of neutrophils than SW620, suggesting that neutrophil-tumour subpopulations interactions vary in response to SW480 and SW620. Interestingly, the MIX TME presents an intermediate percentage of neutrophils, suggesting that while SW480 recruits neutrophils, SW620 may inhibit that recruitment. However, the TME percentage of neutrophils does not change during SW480 engraftment, proposing that tumour rejection is not dependent on neutrophil numbers. Surprisingly, the number of neutrophils in the TME of SW620 increases from 1 to 4dpi, suggesting that SW620 are also able to attract neutrophils. Another hypothesis is that SW620 may block neutrophil reverse migration, leading to neutrophil accumulation. Moreover, since this neutrophil increase parallels engraftment efficiency, we can also hypothesised that neutrophils may present a pro-tumour role in response to SW620. According, results showed that the number of neutrophils in the SW480 TME is independent on the number of tumour cells, while in the SW620 TME there is a positive correlation between the number of neutrophils and SW620 tumour cells. Cells can communicate with each other by short/long range signals. Some communication mechanisms require cell-cell contact and therefore are short range, others are cell-cell contact independent and rely on the release of signals to the extracellular environment. Thus, under the hypothesis that the interactions between this pair of CRC cell lines with neutrophils have qualitative differences, it may be speculated that:

- SW480-neutrophils interactions are mediated by paracrine factors and do not require cell-cell contact, being independent on the number of cells within the tumour;
- Interactions between SW620 and neutrophils require cell-cell contact and thus, the number of neutrophils are dependent on the number of tumour cells.

The zebrafish transgenic for neutrophils allowed this detailed information that we have about this population in the different TMEs. However, the transgenic for macrophages is not so reliable and it was only possible to characterize the SW620 TME. Comparing mpeg and tnfa quantifications throughout time, we observed that these populations do not go through quantitatively change, from 1 to 4dpi. Nevertheless, we could observe that the SW620 TME is richer in macrophages than neutrophils at 1dpi as well as 4dpi. Also, it was possible to distinguish two populations of macrophages, $\approx 60\%$ of tnfa negative and $\approx 40\%$ tnfa positive (dbl+), possibly reflecting distinct polarization states⁵⁶. However, both anti- (M1) and pro-tumour (M2b) macrophages may express tnfa, making it impossible to discriminate the function of SW620 TME macrophage populations. The characterisation of macrophages at SW480 TME is crucial to have insights of the macrophage role in tumour engraftment/rejection. Moreover, results suggest that the ratio between neutrophils/macrophages tends to increase along time in SW620 TME (engraftment).

In conclusion, this work allowed a detailed characterization of these intricate interactions between tumour clones that lead us to several speculative hypotheses that can be summarized in our working model (Fig. 3.1).

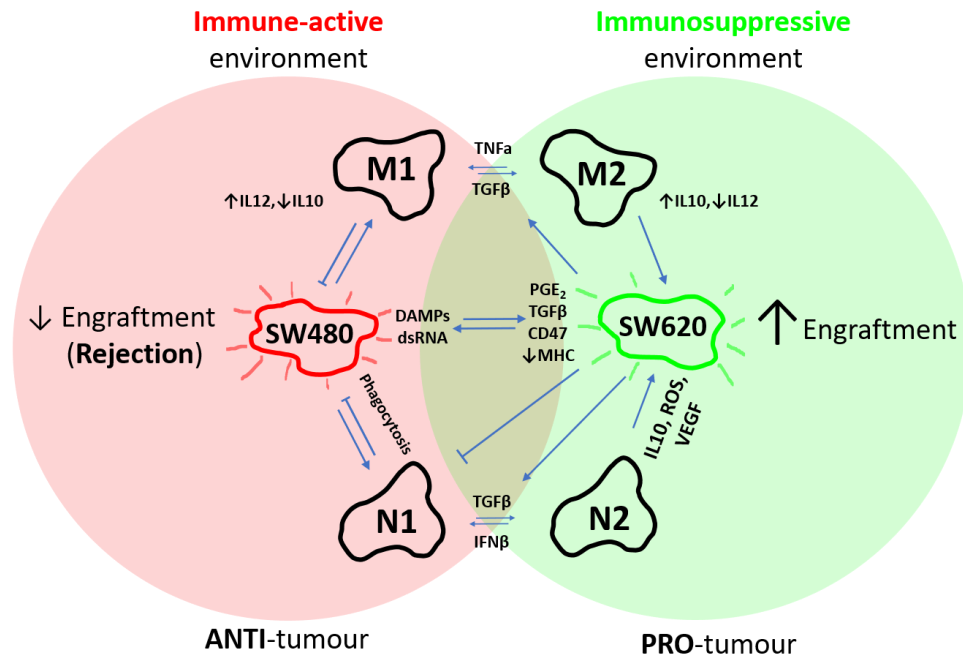


Figure 3.1 **Working hypothesis of the different interactions that may be occurring between innate immune cells and the pair of CRC cell lines during engraftment/rejection:** Cancer subpopulations can induce and be modulated by immune cells in their TME. The immune response to these CRC cell lines may have an anti- or a pro-tumour effect under an immune-active or immunosuppressive microenvironment, respectively, which may involve different markers and signals. It is hypothesised that these distinct interactions between cancer subpopulations and the innate immune response could be the mechanism behind tumour engraftment/rejection.

In this model, SW480 and SW620 have the capacity to interact with each other and with the TME. SW480 seems to be able to recruit more neutrophils and possibly be recognised by macrophages with a phagocytic function, clearing tumour cells and creating an anti-tumour environment, which may prevent the engraftment of SW480 cells (tumour rejection). By contrast, whereas SW480 may recruit anti-tumour neutrophils, SW620 are likely to inhibit this recruitment, evading innate immunity, and possibly polarising neutrophils to a pro-tumour function (N2). Thus, SW620 may create an immunosuppressive environment, evading phagocytic clearance by anti-tumour neutrophils and macrophages. In this TME, innate immune cells acquire a pro-tumour function which favours engraftment efficiency. Both tumour and immune cells are expected to express different markers in response to an anti- or a pro-tumour microenvironment. SW480 may activate innate immunity by the expression of DAMPs, inducing phagocytic neutrophils and macrophages (\uparrow IL12 and \downarrow IL10) to clear the tumour. SW620 may have acquired different mechanisms to not be recognised by innate immunity such as the expression of PGE $_2$, TGF β and CD47 (don't eat me signal). In response to SW620, neutrophils (expressing IL10, ROS and VEGF) and macrophages (expressing low levels of IL12 and high levels of IL10) are prone to a pro-tumoural role.

3.1 A history of clonal evolution according to immunoediting theory

Finally, since SW480 and SW620 illustrate a history of tumour evolution (ie SW480 and SW620 represent two different stages of tumour progression from the same patient: SW480 was derived from the primary tumour and SW620 from a lymph node metastasis 6 month later) we could try to apply an evolution perspective to our results. The SW480 and SW620 co-injection, “MIX”, could represent a third scenario of tumour progression, according to one of these two hypotheses of clonal evolution (Fig. 3.2.A-B):

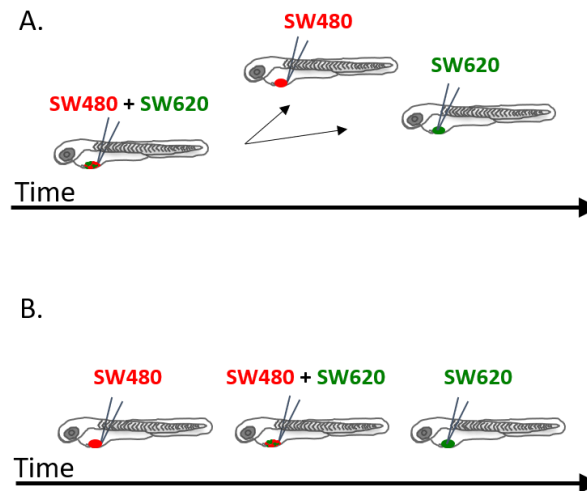


Fig. 3.2 **SW480, SW620 and MIX may represent a history of clonal evolution.** SW480 and SW620 derived from the same patient and represent two stages of tumour progression. Thus, it can be hypothesised whether MIX, co-injection of both cell lines 1:1, could represent a third stage of cancer evolution. According to hypothesis A, MIX could represent an early tumour which presents both subpopulations (SW480 and SW620). During tumour progression, SW480 and SW620 subpopulations diverged from MIX and lead to the primary tumour and metastasis, respectively. Regarding hypothesis B, SW480 represents the primary tumour. This primary tumour acquired a new subpopulation (SW620) and the co-existence of the two subpopulations is represented by MIX. Further, this SW620 subpopulation spread and gave rise to a metastasis.

According to the “immunoediting” theory, during tumour progression, tumours become progressively less immunogenic ie they get less efficient in eliciting an immunological response. Therefore, if we consider the “immunoediting” theory together with Darwinian evolution, we could infer that tumour fitness, ie the tumour that is more able to thrive and progress, is a tumour that has been able to escape immune surveillance and therefore is less immunogenic. Consequently, more advanced stages of tumour progression should be less immunogenic, meaning that are less recognised by the immune system. If the immune system does not recognise tumours, they will present higher implantation capacity when transplanted to an immunocompetent host. Therefore, engraftment capacity could measure tumour fitness. Results show that SW480 engraft poorly, but it is enhanced in the presence of SW620 (MIX), and that SW620 has the highest engraftment capacity. If we consider that the evolution path selects the clones with highest fitness, then the history of clonal evolution described in the hypothesis B is the most likely to have occurred.

3.2 Future Work

All our rational is very speculative and hypothesis driven. However, we can test these hypothesis in the future with several experiments:

1. Test the immunoediting concept in SW480 cells

According to the tumour immunoediting concept, the immune system modulates tumour immunogenicity and only the less immunogenic populations may remain in the host, forming “edited” tumours, which can implant more efficiently³³. This work suggests that SW480 xenotransplants are more heterogeneous with high variability of engraftment and therefore present different intra-immunogenicity. Thus, it is expected that the more immunogenic clones on SW480 xenografts are the ones being rejected by the anti-tumour innate immune response. If this is true, it is expected that engrafted SW480 xenotransplants have low immunogenicity, presenting the capacity to evade the immune-active TME.

This hypothesis can be tested following the same rational of Schreiber experiments. We could isolate engrafted SW480 xenotransplants, “edited” tumours, and re-inject them in *wt* larvae. It is expected that “edited” SW480 tumours will have a higher capacity to engraft efficiently, by evading the anti-tumour innate immunity/creating an immunosuppressive TME and/or by promoting a pro-tumour immune response. As a control, SW480 cells should be also injected in zebrafish larvae with the innate immune system suppressed. In this context, engrafted SW480 will continue to be immunogenic, “un-edited”. Thus, it is expected that, by re-injecting “un-edited” tumours in *wt* larvae, innate cells will have an anti-tumour function, rejecting SW480 xenotransplants.

2. Myeloid tumour microenvironment characterisation *in vivo*

2.1 Characterisation of macrophage TME populations

Our working model already suggests distinct SW480/SW620 interactions with neutrophils. However, to better understand the interactions occurring in the TME, it is also important to characterise the macrophage populations between the different conditions. There are different zebrafish transgenic lines that can be used as an alternative approach to the Tg(mpeg:mCherry tnfa:GFP)⁵⁶ used in this work. The Tg(mfap4:lanYFP-CAAX) allows the analysis of macrophage behaviour during infection and inflammation in zebrafish⁵⁸. In addition, the Tg(irg1:EGFP) was described to allow real time visualisation of macrophage activation in response to the bacterial endotoxin lipopolysaccharide and to xenografted human cancer cells⁵¹.

2.2 Time-lapse movies of cancer-innate immune cells interactions

To further characterise the neutrophils and macrophages in the TME it is important to analyse their behaviours in response to SW480 or SW620. Yi Feng *et al* characterised the behaviour of immune cells in response to oncogenic transformed cells by time-lapse movies in which different parameters were quantified such as: retention time of immune cells, migration and velocity¹⁵. Under the working model, it is expected that neutrophils and macrophages acquire different functions in response to SW480 (anti-tumour) or SW620 (pro-tumour). The analysis of time-lapse movies of these immune-subclones interactions may allow to further discriminate immune functions between the two TME. As an example, it would be expected to have more phagocytosis in response to SW480 than to SW620.

3. Neutrophil and macrophage immunomodulation

To uncover the mechanism behind engraftment/rejection, it is fundamental to perform loss- and gain-of-function experiments in order to address the role of neutrophil and macrophage populations in the tumour implantation/rejection process.

By taking advantage of mutant zebrafish lines, it is expected that, whenever an immune population responsible for tumour rejection (anti-tumour function) is ablated, the engraftment capacity

of a cell line usually rejected will increase. On the other hand, a reduction on engraftment efficiency should be observed whenever a cell population crucial (pro-tumour function) to this process is ablated. This could be tested by injecting SW480, SW620 and MIX in the *runx*^{W84X} mutant zebrafish line (low neutrophils and high macrophages) and in the *pu.1*^{G242D} mutants (high neutrophils but low macrophages)⁵⁹. Thus, engraftment studies with these mutant lines could unravel the myeloid key cell in tumour implantation.

Another technique to specifically ablate myeloid lineages takes advantage of the UAS:Gal4 and the nitroreductase gene (*nfsB*) system. The nitroreductase converts the pro-drug metronidazole to a cytotoxic metabolite and can be used to ablate specific cell populations in the zebrafish. By crossing a transgenic line expressing *nfsB*:mCherry under the UAS promoter with, for example a Tg(*lyz*:Gal4), it is possible to specifically ablate the neutrophil populations. To ablate macrophage populations, it could be used the Tg(*fms*:Gal4) zebrafish line⁶⁰. By crossing these lines, the nitroreductase (UAS) is expressed in specific cell populations and, upon metronidazole treatment, the *nfsB* kills the cells where it is expressed. One advantage of this approach is that cell populations are only ablated upon metronidazole treatment, meaning that it is possible to ablate cell populations at different time-windows⁶¹.

4. Transcriptome analysis

To go further and unravel the molecules behind engraftment/rejection, the transcriptome of cells involved in rejection should be compared with the transcriptome of cells associated with an implantation prone microenvironment. In other words, it is expected that the transcriptome of tumour and TME immune cells would change either in response to anti- or pro-tumour environmental cues. In our working hypothesis, possible molecules that may be associated with an anti-tumour (SW480) and with a pro-tumour (SW620) are described. RNAseq analysis of SW480 and SW620, both tumour and TME cells, could highlight the main molecules and pathways that may be involved in engraftment/rejection. In addition to these, the transcriptome of “un-edited” and “edited” SW480 could also give insights of the molecules and pathways involved in rejection (anti-tumour) and engraftment (pro-tumour/immunosuppressive TME). Finally, the necessity and sufficiency of the main candidate molecules/pathways should be tested by loss- and gain-of-function experiments.

Overall, these experiments could clarify the mechanism behind engraftment/rejection and drive new insights about the immunoediting process that modulates tumour progression. The study of these immune mechanisms may unravel different/new pathways to block the tumour immunosuppressive microenvironment, highlighting new and complementary targets for immunotherapies⁶². Then again, discovering molecules that suppress rejection may improve the engraftment efficacy of xenotransplants, which can be used as a screening platform for personalised medicine.

4. Materials and Methods

4.1 Experimental outline

This work required previous preparation of immortalised cell lines, as well as the preparation of the distinct transgenic and mutant zebrafish lines. The experimental outline is described as follows in figure 4.1.

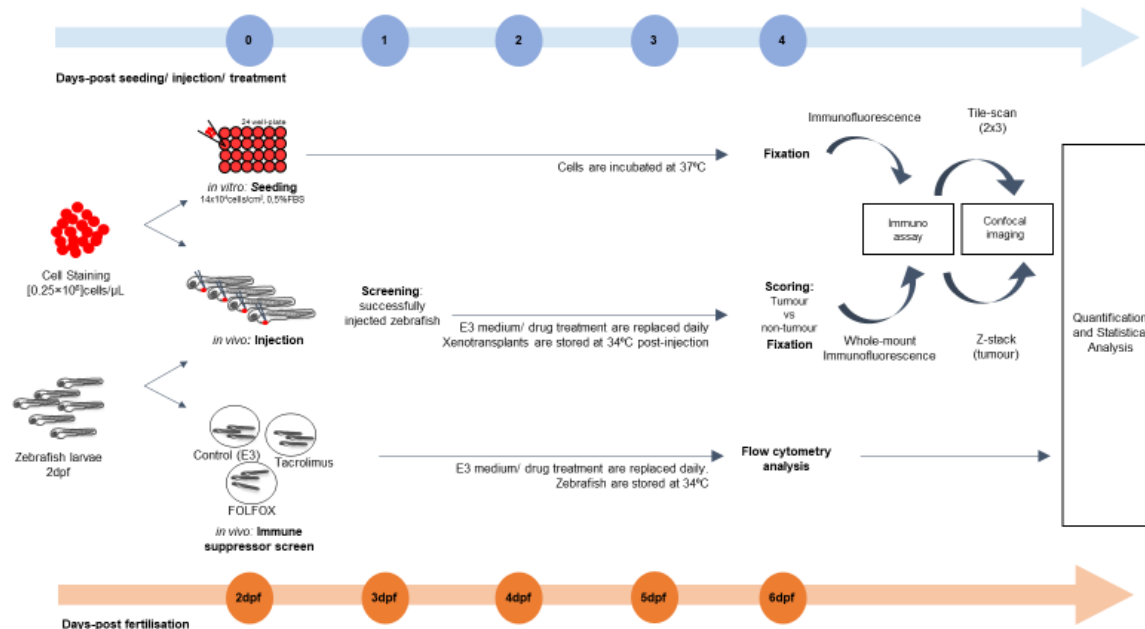


Figure 4.1 **Experimental outline.** This work comprised *in vitro* and *in vivo* experiments. For the *in vitro* part, human CRC cell lines were previously stained with a fluorescent dye and seeded at 14×10^4 cells/cm² in 24-well plates. Cells were incubated at 37°C for 4 days. In the *in vivo* setting two different experiments were performed: a xenotransplantation of human CRC cell lines and an immune suppressor screen. The xenotransplantation consisted in the microinjection of cancer cell lines in the PVS of 2dpf larvae. In the next day, all xenotransplants are screened and all unsuccessfully xenotransplants are discarded from the experiment. After 4dpi, all xenografts were scored according to the presence of a tumour and fixed for further analysis. The immune suppressor screen consisted in treating 2dpf transgenic larvae with immunosuppressive drugs for 4days and later immune cell populations (GFP or mCherry) were quantified by flow cytometry. At the end of each experiment, either seeded cells or the xenografts were fixed and stained by an immunofluorescence protocol, imaged by confocal microscopy and quantified.

4.2 Cell Culture

Colon cancer cell lines, SW480 and SW620, originally from American Type Culture Collection (ATCC) were tested for mycoplasma and authenticated through short tandem repeat (STR) profiling. Cells were expanded for 2 weeks before being used in the experiments and were kept in culture for two months (no more than 20 passages). Cells were frozen in liquid nitrogen for long term preservation of cell viability and a batch of several cryovials with few (3-4) number of passages to avoid the acquisition of mutations was saved.

4.2.1 Thawing and expansion of cells

SW480 and SW620 adherent cells were cultured using filtered Dulbecco's Modified Eagle Medium (DMEM) culture medium (Biowest) supplemented with 10% fetal bovine serum (FBS – Gibco and Sigma) and 1% Penicillin-Streptomycin 10,000 Units/mL (Hyclone) in an incubator with humidified atmosphere containing 5% CO₂ at 37°C (inCu Safe). Passage of the cells was performed twice a week once cells achieved a confluence of 70-80%.

4.2.2 Labelling of cell lines

Cells with a confluence of 70%, were washed with DPBS 1x (Gibco; Life Technologies) and stained in a T-flask with a fluorescent dye. Each cell line was stained with different colours to be distinguished when mixed: Vibrant-DiI (red, 4 μ L/mL) and DeepRed (Cy5, 1 μ L/mL) in DPBS – 10 min at 37°C followed by 15min on ice in darkness. Then, both SW480 and SW620 cells were detached with 2mM PBS-EDTA, centrifuged for 4min at 1200rpm and resuspended in DMEM for cell quantification. Cell viability was assessed through trypan blue exclusion method and counted with a haemocytometer. Cells were centrifuged again and resuspended in DPBS to a final cell suspension with concentration of 0.25 $\times 10^6$ cells/ μ L. SW480 and SW620 were then mixed in equal proportions (1:1, “MIX”).

4.3 Zebrafish care and handling

In vivo experiments were performed using the zebrafish (*Danio rerio*) *in vivo* model, which was handled according to European animal welfare regulations and standard protocols. Different genetically modified zebrafish lines were used: Casper, transparent; Tg(fli1:EGFP), labels endothelial cells/blood vessels; Tg(mpx:GFP), labels neutrophils and Tg(mpeg:mCherry tnfa:GFP), labels macrophages and tnfa⁺ cells.

Adult zebrafish were kept in 3.5L tanks with running water, with a maximum population of 30 fish per tank. Each tank had both male and female fish and they were fed twice a day by the fish facility staff.

4.3.1 Crossing and housing of adult zebrafish and embryo harvesting

The zebrafish used for the experiments were 2dpf. To obtain the larvae required for the experiments, adult zebrafish were crossed three days in advance. Crosses took place into slopping breeding tanks that allow the eggs to fall, while preventing the adults from eating them. Both the slope that mimics the shallow waters where zebrafish mate in their natural habitat and the synthetic algae were used in the breeding tanks to improve environment enrichment. Adult zebrafish mate in the morning and after the cross, they are transferred back to their original tanks. The embryos are harvested and incubated in petri dishes with embryo medium (E3) (≈ 50 embryos per Petri dish) at 28°C for the next 2days.

4.4 Experiments - *in vitro* assay

4.4.1 Seeding

Cells were seeded in 24 well-plates with a coverslip (VWR Borosilicate cover glass, 13mm diameter, Thickness no.1.5) inserted in each well. Upon cell labelling, cells were diluted in DMEM (supplement with 0.5%FBS Gibco) to a concentration of 6 $\times 10^4$, 10 $\times 10^4$ and 14 $\times 10^4$ cells/cm² in a final volume of 500 μ L/well. The plates were incubated in a humidified atmosphere for 4 days (to be comparable with the *in vivo* xenotransplants) containing 5% CO₂ at 37°C. Cells were fixed with 4% PFA for 10min at room temperature and then washed out with DPBS.

4.4.2 Immuno fluorescence technique

Cells were permeabilised with PBS triton 0.1% (10 min) and left for 60 min in a blocking solution (containing bovine serum albumin (BSA), PBS 1X, Triton and goat serum). Then, the coverslips were incubated overnight with primary antibodies (1:200) diluted in the same reagent previously used in a humid chamber at 4°C.

On the next day, the coverslips were inserted back into 24 well plates, washed with blocking solution (3x5min) and incubated with secondary antibodies (1:500) in blocking solution for 60min at room temperature with slow shaking. Then, coverslips were washed with DPBS (2x5min) and 150 μ L/well of 4',6-diamidino-2-phenylindole (DAPI) solution (15 μ L of stock DAPI (5mg/ml) in 10mL

H2O) were added (10min) to stain cell nuclei. Finally, the coverslips were carefully dried, mounted on top of glass slides with a small drop of mounting medium (DAKO) and stored at 4°C.

4.5 Experiments - Injections of tumour cells in zebrafish larvae

4.5.1 Zebrafish Xenografts

Fluorescent-labelled cells were microinjected into the PVS of anaesthetised (Tricaine 1x) 2dpf larvae under a fluorescence microscope. After injection, xenografts were transferred to 34°C until the end of the experiment, a compromised temperature between the optimal temperature for human cells growth and zebrafish correct development. E3 medium or drug treatment were replaced daily and dead larvae were removed. On the following day (1dpi), larvae with cell in the yolk, cell debris or non-injected zebrafish larvae were discarded (screening). Successfully injected zebrafish were kept in the incubator until 4dpi. At this time point larvae were scored according to the presence of tumours into the PVS: 1 – tumour vs 0 – non-tumour. Larvae were then sacrificed (Tricaine 25x) and fixed (PFA 4%, Thermo Scientific) overnight. On the next days, xenografts were stored in Methanol (VWR Chemical) at -20°C for tissue conservation until immunofluorescence.

4.5.2 Whole-mount immunofluorescence

In the first day, xenografts were rehydrated through a methanol series 75%, 50% and 25% until PBS 1X. Then larvae were permeabilised 4x5min with PBS triton 0,1%, washed with sterile water for 5min and incubated in acetone (Fisher Chemicals) for 7min at -20°C. Larvae were washed twice in PBS triton 0.1% and blocked for 1hour at room temperature in a blocking solution. Xenografts were incubated with specific primary antibodies (1:100) in blocking solution (containing BSA, dimethyl sulfoxide (DMSO), PBS 1X, Triton and goat serum) for 1h at room temperature and then overnight at 4°C. On the next day, larvae were washed and permeabilised with 2x10min of PBS triton 0,1% followed by 3x30min PBS tween 0,05% (Fisher Scientific) and incubated with specific secondary antibodies (1:400) and DAPI (nuclei staining, 1:100) in blocking solution for 1h at room temperature and overnight at 4°C. On the third and final day of the immunofluorescence assay, the larvae were washed 4x15min in PBS tween 0,05% and fixed with PFA 4%. Xenografts were mounted in mounting media (Dako) into coverslips for microscopy observation and stored at 4°C.

4.6 Confocal Microscopy

Tumour cells were imaged in a Zeiss LSM 710 fluorescence confocal microscope at 40x magnification and quantified with the Cell Counter plugin ImageJ software (v. 1.44). Xenograft sequential images along the tumour's depth with a 5µm interval were obtained using the z-stack function. Three z-stack slices (Zfirst, Zmiddle, Zlast) per xenotransplants were analysed and then, the total cell number (DAPI nuclei stain) of the entire tumour was estimated – average (AVG) of the 3 slices x total number of slices/1,5 (constant that we use upon observation that between 2 slices there's a common share of half of the cells from the next slice).

In vitro tumour cells were randomly imaged using the tile-scan (2x3) confocal function, avoiding the centre and the periphery of the coverslip. Three technical replicates were analysed – each coverslip is represented by the mean of the quantification of six tile-scan images.

The number of injected cells per fish was the same in both controls and in the mix, thus, the number of each cell type injected per fish in the mix was only half of the same cell type injected per fish in the corresponding control. Therefore, to be comparable with SW480 and SW620 total cell number when mixed, the total cell number of SW480 and SW620 when cultured/injected alone was normalised by dividing the total cell number by 2. Apoptotic cells, proliferative cells, neutrophils and macrophages were divided by total cell number and analysed as a percentage.

4.7 Statistical analysis

Statistical analysis was performed using the GraphPad Prism software (v. 6.05 for Windows). All data were challenged by two normality tests: the D'Agostino & Pearson normality test and the Shapiro-Wilk normality test. A Gaussian distribution was assumed only for datasets that pass the two normality tests and were analysed by unpaired *t* test. Datasets that do not pass the normality test were analysed by the Mann-Whitney test. Differences were considered significant at $P < 0.05$. Whenever the number of independent experiments was small, differences were compared using a Z-test considering the number of samples.

4.8 Experiments - Immune suppressor screen

4.8.1 Zebrafish larvae drug administration

The 2dpf zebrafish larvae were randomly distributed to the treatment groups: control in E3 medium, FOLFOX in E3 (4.2 mM 5-FU, 0.18mM folinic acid, 0.08 mM oxaliplatin) and Tacrolimus in E3 (0.0578 μ M). The maximum drug concentration tolerated by zebrafish larvae was previously tested using as reference the maximum patient's plasma concentration for each compound. E3 medium control (between 2-6dpf), FOLFOX (3-6dpf) and Tacrolimus (2-6dpf) were replaced daily.

4.8.2 Flow cytometry analysis

Zebrafish larvae were sacrificed at 6dpf (Tricaine 25x) and 50 larvae per condition were transferred to a 1,5mL eppendorf and washed with DPBS (3x). An enzymatic digestion of zebrafish tissues was performed by adding Liberase (10 μ L/ml) to the eppendorf tubes at 28°C for 1.5-2hours in slow agitation. To speed up larval tissue disaggregation, temperature was increased to 37°C and larvae were frequently resuspended. Cell suspension was filtered using CellTrics® 40 μ m filters to avoid cell clumping, directly to a cytometer tube. PBS was added and the suspension was centrifuged at 300G for 10 min at 4°C. Finally, supernatants were discarded, cells were resuspended in 500 μ L of DPBS 1x and immediately analysed by flow cytometry. Casper and runx^{w84x} were used as non-fluorescent controls. Flow cytometry analysis was performed using a LSRFortessa™ X-20 (BD Biosciences) and data analysed using FlowJo 10.3.0 software (BD Biosciences). Differences between groups were tested using a paired non-parametric Wilcoxon test in the Graph Prism software.

5. References

1. Hanahan, D. & Weinberg, R. A. Hallmarks of cancer: The next generation. *Cell* **144**, 646–674 (2011).
2. Burrell, R. A., Mcgranahan, N., Bartek, J. & Swanton, C. The causes and consequences of genetic. *Nature* **503**, (2013).
3. Almendro, V., Marusyk, A. & Polyak, K. Cellular heterogeneity and molecular evolution in cancer. *Annu Rev Pathol* **8**, 277–302 (2013).
4. Nowell, P. C. The Clonal Evolution of Tumor Cell Populations. *Science (80-.)*. **194**, 23–28 (1950).
5. Greaves, M. & Maley, C. C. Clonal evolution in cancer. *Nature* **481**, 306–13 (2012).
6. American Cancer Society. Oncogenes and tumor suppressor genes. Available at: (<https://www.cancer.org/cancer/cancer-causes/genetics/genes-and-cancer/oncogenes-tumor-suppressor-genes.html>). (Accessed: 1st November 2017)
7. Tomasi, T. B. & Magner, Æ. W. J. Epigenetic regulation of immune escape genes in cancer. *Cancer Immunol. Immunother.* **55**, 1159–1184 (2006).
8. Caiado, F. & Silva-santos, B. Intra-tumour heterogeneity – going beyond genetics. *FEBS J.* **283**, 2245–2258 (2016).
9. Mcgranahan, N. & Swanton, C. Review Clonal Heterogeneity and Tumor Evolution : Past , Present , and the Future. *Cell* **168**, 613–628 (2017).
10. Cleary, A. S., Leonard, T. L., Gestl, S. A. & Gunther, E. J. Tumour cell heterogeneity maintained by cooperating subclones in Wnt-driven mammary cancers. *Nature* **508**, 113–117 (2014).
11. Polyak, A. M. and K. Tumor heterogeneity: causes and consequences. *Biochim Biophys Acta* **1805**, 1–28 (2011).
12. Pattabiraman, D. R. & Weinberg, R. A. Tackling the cancer stem cells — what challenges do they pose? *Nat. Publ. Gr.* **13**, 497–512 (2014).
13. Quail, D. F. & Joyce, J. A. Microenvironmental regulation of tumor progression and metastasis. *Nat. Med.* **19**, 1423–37 (2013).
14. Quail, D. F. *et al.* The tumor microenvironment underlies acquired resistance to CSF-1R inhibition in gliomas. *Science (80-.)*. **352**, (2016).
15. Feng, Y., Santoriello, C., Mione, M., Hurlstone, A. & Martin, P. Live Imaging of Innate Immune Cell Sensing of Transformed Cells in Zebrafish Larvae : Parallels between Tumor Initiation and Wound Inflammation. *PLOS Biol.* **8**, (2010).
16. Parcesepe, P., Giordano, G., Laudanna, C., Febbraro, A. & Pancione, M. Cancer-Associated Immune Resistance and Evasion of Immune Surveillance in Colorectal Cancer. *Gastroenterol. Res. Pract.* **2016**, (2016).
17. Gentles, A. J. *et al.* The prognostic landscape of genes and infiltrating immune cells across human cancers. *Nat. Med.* **21**, (2015).
18. Plebanek, M. P. *et al.* Pre-metastatic cancer exosomes induce immune surveillance by patrolling monocytes at the metastatic niche. *Nat. Commun.* **8**, (2017).
19. Marcus, A. *et al.* Recognition of tumors by the innate immune system and natural killer cells.

- NIH* **122**, 1–33 (2015).
20. Feng, Y., Renshaw, S., Martin, P., Court, F. & Bank, W. Report Live Imaging of Tumor Initiation in Zebrafish Larvae Reveals a Trophic Role for Leukocyte-Derived PGE 2. *CURBIO* **22**, 1253–1259 (2012).
 21. Fridlender, Z. G. *et al.* Article Polarization of Tumor-Associated Neutrophil Phenotype by TGF- b : “ N1 ” versus “ N2 ” TAN. *Cancer Cell* **16**, 183–194 (2009).
 22. Oliveira, S. De, Reyes-aldasoro, C. C., Candel, S. & Stephen, A. Cxcl8 (Interleukin-8) mediates neutrophil recruitment and behavior in the zebrafish inflammatory response. *Eur. PMC Funders Gr.* **190**, 4349–4359 (2013).
 23. Oliveira, S. De, Rosowski, E. E. & Huttenlocher, A. Neutrophil migration in infection and wound repair : going forward in reverse. *Nat. Publ. Gr.* **16**, 378–391 (2016).
 24. Selders, G. S., Fetz, A. E., Radic, M. Z. & Bowlin, G. L. An overview of the role of neutrophils in innate immunity , inflammation and host-biomaterial integration. *Regen. Biomater.* **4**, 55–68 (2017).
 25. Chanmee, T., Ontong, P., Konno, K. & Itano, N. Tumor-Associated Macrophages as Major Players in the Tumor Microenvironment. *Cancers (Basel)*. **6**, 1670–1690 (2014).
 26. Kannegieter, N. M. *et al.* The Effect of Tacrolimus and Mycophenolic Acid on CD14+ Monocyte Activation and Function. *PLoS One* **12**, 1–19 (2017).
 27. Zhang, M. *et al.* A high M1 / M2 ratio of tumor-associated macrophages is associated with extended survival in ovarian cancer patients. *J. Ovarian Res.* **7**, 1–16 (2014).
 28. Vincent, W. J. B., Harvie, E. A., Sauer, J. & Huttenlocher, A. Neutrophil derived LTB4 induces macrophage aggregation in response to encapsulated Streptococcus iniae infection. *PLoS One* **12**, 1–16 (2017).
 29. Nausch, N., Galani, I. E., Schlecker, E. & Cerwenka, A. Mononuclear myeloid-derived ‘ suppressor ’ cells express RAE-1 and activate natural killer cells. *Blood* **112**, 4080–4090 (2016).
 30. Smyth, B. M. J. *et al.* Differential Tumor Surveillance by Natural Killer (NK) and NKT Cells. *J. Exp. Med.* **191**, (2000).
 31. Biroccio, A. *et al.* TRF2 inhibits a cell-extrinsic pathway through which natural killer cells eliminate cancer cells. *Nat. Cell Biol.* **15**, 818–828 (2013).
 32. Grivnennikov, S. I., Greten, F. R. & Karin, M. Immunity, Inflammation, and Cancer. *Cell* **140**, 883–899 (2010).
 33. Schreiber, R. D., Old, L. J. & Smyth, M. J. Cancer immunoediting : Integrating immunity’s roles in cancer suppression and promotion. *Science (80-.).* **331**, (2011).
 34. Kaplan, D. H. *et al.* Demonstration of an interferon y-dependent tumor surveillance system in immunocompetent mice. *PNAS* **95**, (1998).
 35. Vesely, M. D., Kershaw, M. H., Schreiber, R. D. & Smyth, M. J. Natural Innate and Adaptive Immunity to Cancer. *Annu. Rev. Immunol.* **29**, (2011).
 36. Nakayama, M. *et al.* IFN-g is required for cytotoxic T cell-dependent cancer genome immunoediting. *Nat. Commun.* **8**, 1–13 (2017).
 37. Sullivan, T. O. *et al.* Cancer immunoediting by the innate immune system in the absence of adaptive immunity. *J. Exp. Med.* **209**, 1869–1882 (2012).
 38. Dupage, M. *et al.* Endogenous T Cell Responses to Antigens Expressed in Lung

- Adenocarcinomas Delay Malignant Tumor Progression. *Cancer Cell* **19**, 72–85 (2011).
39. Dupage, M., Mazumdar, C., Schmidt, L. M., Cheung, A. F. & Jacks, T. Expression of tumour-specific antigens underlies cancer immunoediting. *Nature* **482**, 405–409 (2012).
 40. Matsushita, H. *et al.* Cancer Exome Analysis Reveals a T Cell Dependent Mechanism of Cancer Immunoediting. *Nature* **482**, 400–404 (2013).
 41. Dighe, A. S., Richards, E., Old, L. J. & Schreiber, R. D. Enhanced In Vivo Growth and Resistance to Rejection of Tumor Cells Expressing Dominant Negative IFN γ Receptors. **1**, 447–456 (1994).
 42. Diamond, M. S. *et al.* Type I interferon is selectively required by dendritic cells for immune rejection of tumors. *J. Exp. Med.* **208**, 1989–2003 (2011).
 43. Shankaran, V. *et al.* IFN γ and lymphocytes prevent primary tumour development and shape tumour immunogenicity. *Nature* **410**, 1107–1111 (2001).
 44. Dunn, G. P., Bruce, A. T., Ikeda, H., Old, L. J. & Schreiber, R. D. Cancer immunoediting : from immuno-surveillance to tumor escape. *Nat. Immunol.* **3**, 991–998 (2002).
 45. Fior, R. *et al.* Single-cell functional and chemosensitive profiling of combinatorial colorectal therapy in zebrafish xenografts. *PNAS* **114**, (2017).
 46. Trede, N. S., Langenau, D. M., Traver, D., Look, A. T. & Zon, L. I. The use of zebrafish to understand immunity. *Immunity* **20**, 367–379 (2004).
 47. Medzhitov, R. & Jr, C. A. J. Decoding the Patterns of Self and Nonself by the Innate Immune System. *Science (80-.)*. **298**, 10–13 (2012).
 48. Keith Roberts, Dennis Bray, Julian Lewis, Martin Raff, Alexander Johnson, B. A. *Molecular Biology of the cell*. (Garland Science, 2014).
 49. Robertson, A. L., Avagyan, S., Gansner, J. M. & Zon, L. I. Understanding the regulation of vertebrate hematopoiesis and blood disorders: big lessons from a small fish. *FEBS Lett.* 1–18 (2016). doi:10.1002/1873-3468.12415
 50. Zon Laboratory. Vertebrate Hematopoiesis and Zebrafish Development. Available at: <https://zon.tchlab.org/?p=463>.
 51. Sanderson, L. E. *et al.* An inducible transgene reports activation of macrophages in live zebrafish larvae. *Dev. Comp. Immunol.* **53**, 63–69 (2015).
 52. Shiao, C. E., Kaufman, Z., Meireles, A. M. & Talbot, W. S. Differential Requirement for irf8 in Formation of Embryonic and Adult Macrophages in Zebrafish. *PLoS One* **10**, 1–15 (2015).
 53. Jing, L. & Zon, L. I. Zebrafish as a model for normal and malignant hematopoiesis. *Dis. Model. Mech.* **4**, 433–438 (2011).
 54. Tian, Y. *et al.* The first wave of T lymphopoiesis in zebrafish arises from aorta endothelium independent of hematopoietic stem cells. *J. Exp. Med.* **11**, 1–14 (2017).
 55. Page, D. M. *et al.* An evolutionarily conserved program of B-cell development and activation in zebra fish. *Blood* **122**, 1–12 (2016).
 56. Travnickova, J. *et al.* Identification of polarized macrophage subsets in zebrafish. *Elife* **4**, 1–14 (2015).
 57. Gajewski, T. F., Schreiber, H. & Fu, Y.-X. Innate and adaptive immune cells in the tumor microenvironment. *Nat. Immunol.* **14**, 1014–22 (2013).
 58. Walton, E. M., Cronan, M. R., Beerman, R. W. & Tobin, D. M. The Macrophage-Specific

- Promoter mfap4 Allows Live , Long-Term Analysis of Macrophage Behavior during Mycobacterial Infection in Zebrafish. *PLoS One* **10**, 1–17 (2015).
59. Jin, H. *et al.* Runx1 regulates embryonic myeloid fate choice in zebrafish through a negative feedback loop that confines Pu.1 expression. *Blood* **119**, (2012).
60. Prajsnar, T. K. *et al.* A privileged intraphagocyte niche is responsible for disseminated infection of *Staphylococcus aureus* in a zebrafish model. **14**, 1600–1619 (2012).
61. Mathias, J. R., Zhang, Z., Saxena, M. T. & Mumm, J. S. Enhanced Cell-Specific Ablation in Zebrafish Using a Triple Mutant of *Escherichia Coli* Nitroreductase. *Zebrafish* **11**, 85–97 (2014).
62. Sharma, P. & Allison, J. P. Immune Checkpoint Targeting in Cancer Therapy : Toward Combination Strategies with Curative Potential. *Cell* **161**, 205–214 (2015).